NAVAL POSTGRADUATE SCHOOL
Monterey, California

THESIS

MESOSCALE SURFACE ANALYSES OF THE ERICA IOP-2 CYCLONE

by

Craig D. Lilly

December 1990

Thesis Advisor Wendell A. Nuss

Approved for public release; distribution is unlimited.

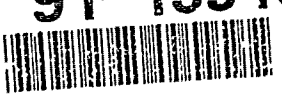

Unclassified

security classification of this page

REPORT DOCUMENTATION PAGE

1a Report Security Classification Unclassified			1b Restrictive Markings
2a Security Classification Authority			3 Distribution/Availability of Report
2b Declassification/Downgrading Schedule			Approved for public release; distribution is unlimited.
4 Performing Organization Report Number(s)			5 Monitoring Organization Report Number(s)
6a Name of Performing Organization Naval Postgraduate School	6b Office Symbol *(if applicable)* 35		7a Name of Monitoring Organization Naval Postgraduate School
6c Address *(city, state, and ZIP code)* Monterey, CA 93943-5000			7b Address *(city, state, and ZIP code)* Monterey, CA 93943-5000
8a Name of Funding/Sponsoring Organization	8b Office Symbol *(if applicable)*		9 Procurement Instrument Identification Number
8c Address *(city, state, and ZIP code)*			10 Source of Funding Numbers
			Program Element No / Project No / Task No / Work Unit Accession No

11 Title *(include security classification)* MESOSCALE SURFACE ANALYSES OF THE ERICA IOP-2 CYCLONE

12 Personal Author(s) Craig D. Lilly

13a Type of Report	13b Time Covered	14 Date of Report *(year, month, day)*	15 Page Count
Master's Thesis	From To	December 1990	77

16 Supplementary Notation The views expressed in this thesis are those of the author and do not reflect the official policy or position of the Department of Defense or the U.S. Government.

17 Cosati Codes			18 Subject Terms *(continue on reverse if necessary and identify by block number)*
Field	Group	Subgroup	rapid cyclogenesis, surface fluxes, boundary layer

19 Abstract *(continue on reverse if necessary and identify by block number)*

The mesoscale structure of an explosively deepening open-ocean cyclone, the Intensive Observation Period (IOP) #2 of the Experiment on Rapidly Intensifying Cyclones over the Atlantic (ERICA) which occurred 13-14 December 1988, was studied. Aircraft, buoy and ship observations were plotted in 3 h blocks, and detailed hand-analyses of surface pressure and temperature, as well as frontal and cyclone structure, were prepared. The analyses were then converted to a 20 km grid using a Cressman analysis scheme, and the gridded fields passed to a Brown-Liu planetary boundary layer (PBL) model to calculate surface latent and sensible heat fluxes. The results of the mesoscale surface analysis showed that the regions east and northeast of the low featured less warm thermal advection than expected for a typical maritime cyclone and a low-level easterly flow that had a 5-10°C thermal disequilibrium between the sea surface and the overlying air. This caused substantial positive heat fluxes east of the low throughout the 12 h prior to and during rapid deepening. This pattern of surface interaction is substantially different from other cyclones and suggests that surface processes contributed significantly to the cyclogenesis

20 Distribution/Availability of Abstract	21 Abstract Security Classification	
☒ unclassified/unlimited ☐ same as report ☐ DTIC users	Unclassified	
22a Name of Responsible Individual Wendell A. Nuss	22b Telephone *(include Area code)* (408) 646-3275	22c Office Symbol MR(Nu)

DD FORM 1473,84 MAR 83 APR edition may be used until exhausted
All other editions are obsolete

security classification of this page

Unclassified

Approved for public release; distribution is unlimited.

Mesoscale Surface Analyses of the ERICA IOP-2 Cyclone

by

Craig D. Lilly
Lieutenant Commander, United States Navy
B.S., University of California, Davis, 1974

Submitted in partial fulfillment of the
requirements for the degree of

MASTER OF SCIENCE IN METEOROLOGY AND PHYSICAL OCEANOGRAPHY

from the

NAVAL POSTGRADUATE SCHOOL
December 1990

Author: _____
Craig D. Lilly

Approved by: _____
Wendell A. Nuss, Thesis Advisor

_____
Carlyle H. Wash, Second Reader

_____
Robert L. Haney, Chairman,
Department of Meteorology

ABSTRACT

The mesoscale structure of an explosively deepening open-ocean cyclone, the Intensive Observation Period (IOP) #2 of the Experiment on Rapidly Intensifying Cyclones over the Atlantic (ERICA) which occurred 13-14 December 1988, was studied. Aircraft, buoy and ship observations were plotted in 3 h blocks, and detailed hand-analyses of surface pressure and temperature, as well as frontal and cyclone structure, were prepared. The analyses were then converted to a 20 km grid using a Cressman analysis scheme, and the gridded fields passed to a Brown-Liu planetary boundary layer (PBL) model to calculate surface latent and sensible heat fluxes. The results of the mesoscale surface analysis showed that the regions east and northeast of the low featured less warm thermal advection than expected for a typical maritime cyclone and a low-level easterly flow that had a 5-10°C thermal disequilibrium between the sea surface and the overlying air. This caused substantial positive heat fluxes east of the low throughout the 12 h prior to and during rapid deepening. This pattern of surface interaction is substantially different from other cyclones and suggests that surface processes contributed significantly to the cyclogenesis.

TABLE OF CONTENTS

I. INTRODUCTION 1

II. BACKGROUND 3
- A. UPPER LEVEL FORCING AND BOUNDARY LAYER PROCESSES ... 3
- B. LATENT HEAT RELEASE AND SURFACE FLUXES 4
- C. AGEOSTROPHIC CIRCULATION AND FRONTAL CONVERGENCE . 5
- D. VERTICAL AND SLANTWISE MOIST CONVECTION 6
- E. PERIOD OF MAXIMUM INFLUENCE OF SURFACE FLUXES 7
- F. OBJECTIVES 8

III. DATA COLLECTION AND ANALYSIS METHODOLOGY 10
- A. DATA COLLECTION 10
- B. DATA REDUCTION 12
- C. HAND-ANALYSIS OF DATA 13
- D. CRESSMAN ANALYSIS OF IOP-2 DATA 14
- E. FLUX CALCULATIONS IN PLANETARY BOUNDARY LAYER 14

IV. SYNOPTIC DISCUSSION OF IOP-2 20
- A. 0000 - 1200 UTC 13 DECEMBER 1988 20
- B. 1500 - 1800 13 DECEMBER 1988 22
- C. 2100 UTC 13 DECEMBER - 0000 UTC 14 DECEMBER 1988 22
- D. 0300 - 0600 UTC 14 DECEMBER 1988 23
- E. 0900 - 1200 UTC 14 DECEMBER 1988 24
- F. SUMMARY OF DEVELOPMENT 25

V. ANALYSIS OF IOP-2 SURFACE FLUXES 44

VI. CONCLUSIONS 62

VII. RECOMMENDATIONS 63

LIST OF REFERENCES 64

INITIAL DISTRIBUTION LIST 67

LIST OF TABLES

Table 1. SUMMARY OF SURFACE DATA POINTS COLLECTED 11
Table 2. SUMMARY OF DEVELOPMENT OF IOP-2 26
Table 3. WARM SECTOR AIR-SEA TEMPERATURE DIFFERENCES AND HEAT FLUXES 46

LIST OF FIGURES

Fig. 1. Map of ERICA buoy pattern 18
Fig. 2. SST Analysis for 14-16 December 1988 19
Fig. 3. FNOC NOGAPS Analysis for 13/0000 UTC December 1988 27
Fig. 4. GOES IR imagery for 13/1231 UTC December 1988 28
Fig. 5. GOES VIS imagery for 13/1231 UTC December 1988 29
Fig. 6. IOP-2 13/1200 UTC December 1988 mesoscale 30
Fig. 7. IOP-2 13/1500 UTC December 1988 mesoscale 31
Fig. 8. IOP-2 13/1800 UTC December 1988 mesoscale 32
Fig. 9. IOP-2 13/1800 UTC December 1988 surface analysis 33
Fig. 10. IOP-2 13/2100 UTC December 1988 mesoscale 34
Fig. 11. IOP-2 14/0000 UTC December 1988 mesoscale 35
Fig. 12. GOES IR imagery for 14/0031 UTC December 1988 36
Fig. 13. IOP-2 14/0000 UTC December 1988 surface analysis 37
Fig. 14. IOP-2 14/0300 UTC December 1988 mesoscale 38
Fig. 15. GOES IR imagery for 14/0601 UTC December 1988 39
Fig. 16. IOP-2 14/0600 UTC December 1988 mesoscale 40
Fig. 17. GOES IR imagery for 14/1231 UTC December 1988 41
Fig. 18. GOES VIS imagery for 14/1231 UTC December 1988 42
Fig. 19. IOP-2 14/0900 UTC December 1988 mesoscale 43
Fig. 20. Thermal advection at 13/1500 UTC December 1988 51
Fig. 21. Thermal advection at 14/0300 UTC December 1988 52
Fig. 22. Surface level winds and isobars for 13/2100 UTC December 53
Fig. 23. 3 h change in surface temperature (13/1500 -13/1800 UTC) 54
Fig. 24. Time-rate of change of air-sea temperature differences 55
Fig. 25. Sensible heat fluxes for 13/1200 UTC 56
Fig. 26. Latent heat fluxes for 13/1200 UTC 57
Fig. 27. Sensible heat fluxes for 13/1800 UTC 58
Fig. 28. Latent heat fluxes for 13/1800 UTC 59
Fig. 29. Sensible heat fluxes for 14/0600 UTC 60
Fig. 30. Latent heat fluxes for 14/0600 UTC 61

ACKNOWLEDGMENTS

This project has been a team effort at every stage. I would like to thank Russ Schwanz for his patience while teaching me about the IDEA Lab, and Randy Pauley, for the tremendous amount of skillful computer work he did in support of this project. It could never have been completed without their help. Professor Chuck Wash's careful reading and insightful comments greatly improved the clarity of the ideas presented in this paper. I would like to thank in particular Professor Wendell Nuss for originating this project and for his guidance, support, and patience at every turn.

My parents, Wallis and Sheila Crow, have been a source of inspiration and unfailing encouragement from the beginning. My deepest appreciation, of course, goes to my wife Leslie and my daughters Rachel and Sara. Your love and forbearance during nine sets of finals and the thesis crunch have meant more to me than I can ever say.

I. INTRODUCTION

Maritime cyclones are of special interest because of their great capacity to disrupt commerce and cause destruction of property and loss of life at sea. Rapidly deepening maritime cyclones are of particular interest due to the suddenness with which they develop, their intensity and the inability of numerical models to forecast them accurately. They are predominantly cold-season events, and ones which develop most often in a limited mid-latitude zone of the western boundary regions of the Atlantic and Pacific Oceans. Interest in these storms was first sparked by Sanders and Gyakum (1980), who defined explosive cyclogenesis (or the "bomb") as an extratropical surface cyclone whose 24 h central pressure falls averaged at least 1 Bergeron (B), or 24 mb x $\frac{\sin \phi}{\sin 60^\circ}$, where ϕ is the latitude position of the cyclone center midway through the 24-h period. They pointed out that in one sample period in 1978-79, 31 out of 38 of the deepest lows (960 mb or deeper) were rapid deepeners. The problem was that the numerical weather prediction models then available were failing to predict the magnitude of these explosively deepening events. There has been some improvement in numerical weather prediction capabilities since that time (Sanders, 1987). However, there continues to be an insufficient understanding of the dynamical processes which contribute to the rapid development. This realization led to the inception of the ERICA project.

ERICA (Experiment on Rapidly Intensifying Cyclones over the Atlantic) was initiated and funded by the Office of Naval Research (ONR) as a broad effort to develop a more complete understanding of explosively deepening over-ocean cyclones. The specific objective of the program (Hadlock and Kreitzberg, 1988) was to determine and understand the fundamental processes occurring in the atmosphere during rapid cyclogenesis, and then to incorporate them into dynamical prediction models with the hope of being able to identify measurable precursors that would lead to making reliable forecasts. The project has involved the participation of numerous academic institutions and government agencies over a period of several years of planning, culminating in the actual field study in the winter of 1988-89.

The experiment focused on the western North Atlantic roughly between Cape Hatteras and Newfoundland, centered on 42.5°N, 65°W. Data was gathered from a network of drifting meteorological buoys, ships of opportunity operating in the area and land stations. When forecasts indicated that a low-pressure system was likely to deepen

explosively, specially configured aircraft (a WP-3D operated by NOAA and an NCAR Electra) were flown out of NAS Brunswick, Maine, and into the cyclone to gather as much flight level and dropwindsonde data as possible in the period of most rapid deepening. This thesis will deal with the results of the second such storm studied, referred to as Intensive Observation Period (IOP) 2, which occurred on 13-15 December 1988.

In order for a low pressure system to develop into a bomb, there must be a particular interaction between the synoptic, mesoscale and boundary layer processes. An understanding of the pattern of heat and moisture fluxes in the boundary layer, which in turn affect static stability in the atmosphere in the developing low, is critical to gaining a more complete understanding of these interactions. The object of this thesis is to describe the time evolution of the mesoscale structure of the IOP-2 cyclone at the surface as well as evaluate the surface heat and moisture fluxes. From this analysis, the possible flux contributions to frontogenesis and cyclogenesis will be discussed.

All available surface observations of the IOP-2 cyclone were incorporated into a detailed hand-analysis of the cyclone at 3-h intervals between 0600 UTC on 13 December 1988 to 1800 UTC on 14 December, paying particular attention to the 2100-1200 period in which the most rapid deepening occurred. The same data was objectively analyzed using a 5-pass Cressman numerical analysis scheme (Cressman, 1959), which converted the basic observations of sea level pressure, temperature, and dew point to grid point analyses on a 20 km grid. The Cressman analyses were then compared to the hand analyses, and the numerical contours adjusted by adding bogus data points to modify the gridded fields toward the hand-analyzed fields. The resulting gridded data sets were then used to determine the surface heat and momentum fluxes by using a modified Brown-Liu planetary boundary layer model (Brown and Liu, 1982).

A review of the relevant literature will be presented in Chapter II. Chapter III will discuss the data and methods of analysis used. A synoptic overview of IOP-2 will be presented in Chapter IV, with a special emphasis on surface-level mesoscale development. Chapter V will discuss the results of the planetary boundary layer analysis of the fluxes and their potential contribution to rapid cyclogenesis. The final chapters will present my conclusions and recommendations for further research.

II. BACKGROUND

Explosive cyclones have a strong tendency to form in western ocean basins in mid-winter, near zones of high sea surface temperature (SST) gradients. Although baroclinic instability is certainly the primary contributor to any developing surface low pressure system, the extraordinary rate of development of a bomb must be the result of some other additional, more subtle factors. Other factors to be investigated are surface fluxes and their influence on frontal convergence and convective stability.

The synoptic forecasting models have consistently underforecast rapid cyclogenesis, which indicates an incomplete understanding of the dynamics of explosive cyclogenesis. These models are reasonably good at forecasting continental cyclogenesis events, as well as the features of the upper-level flow over maritime regions, as Chalfant (1989) found in the case of IOP-2. The success of numerical model forecasts at lower levels has been somewhat less consistent. The operational National Meteorological Center (NMC) Limited-area Fine Mesh (LFM) II model regularly underforecast such intensive maritime developments (Davis and Emanuel, 1988). However, Sanders (1987) has reported improved cyclogenesis forecasts using the NMC Nested Grid Model (NGM).

A. UPPER LEVEL FORCING AND BOUNDARY LAYER PROCESSES

The initial question addressed by researchers was one regarding the relative importance of upper-level forcing versus boundary layer processes in causing explosive deepening. The traditional view is that cyclones develop as the result of baroclinic instability resulting in vertical wind shear associated with upper level jets and weak static stability (Holton, 1979). Reed and Albright (1986) reviewed investigations into two different bombs: the President's Day storm of 18-19 February 1979 and the QE-II storm of 9-10 September 1978. The former cyclone formed under conditions of comparatively strong upper-level forcing due to the presence of a pre-existing upper-level trough. The latter storm formed under a much simpler upper-level flow pattern, implying a lesser degree of forcing at that level. Sanders (1986) found in 48 cases of west-central North Atlantic rapid cyclogenesis that a 500 mb vorticity maximum previously existed upstream of the surface cyclone. Other studies such as Wash et al. (1988) have shown the importance of upper-level forcing on development. However, even with strong baroclinic effects marine boundary layer processes may be important. Indeed, Reed and

Albright (1986) noted the following environmental factors common to the two storms they reviewed:

- Both storms formed over warm waters ($\sim 22°C$).
- Strong SST gradients existed nearby.
- Both were characterized by strong baroclinity.
- Satellite imagery indicated the existence of deep convection in the vicinity of both storm centers.

These factors all suggest that diabatic processes associated with the boundary layer marine environment have a strong influence on rapid cyclogenesis. Such processes are obviously less significant in continental cyclogenesis, where explosive cyclones are not often observed. Nuss and Kamikawa (1990) noted in a comparison of two maritime cyclones, only one of which was a rapid deepener, that strong upper-level forcing associated with jet streak divergence regions caused enhanced vertical motion and cyclogenesis in the case of the explosive cyclone. Chalfant (1989), too, has noted that upper-level processes were a significant factor in the development of the IOP-2 cyclone. What is not clear is the way in which the surface processes interacted with the upper-level forcing in this case to produce an explosive cyclone.

B. LATENT HEAT RELEASE AND SURFACE FLUXES

Investigations into boundary layer processes in rapid cyclogenesis have centered on the role of latent and sensible heat fluxes and thermal advection in low-level static stability. Nuss and Anthes (1987) conducted a numerical investigation into an idealized cyclone's sensitivity to surface heat and moisture fluxes. Using a Pennsylvania State University (PSU)/National Center for Atmospheric Research (NCAR) baroclinic channel-flow model and realistic physics, they tested the sensitivity of cyclogenesis to a variety of different environmental conditions, such as:

- No surface heat fluxes.
- A sinusoidal wave in the SST gradient.
- No latent heat release.
- High and low static stability.
- Less intense temperature gradients.

They found that baroclinic instability is sufficient to lead to rapid cyclogenesis, and that the rate of development is sensitive to a number of factors. The most significant factors were the effects of surface heat and moisture fluxes, which varied from reducing

the rate of cyclogenesis by 25% to increasing the rate by 15%, depending on the distribution of surface fluxes in the cyclone. They found that when a sinusoidal SST gradient was in phase with the low level thermal wave such that there was heating to the east and northeast of the surface low the atmosphere produced upward heat and moisture fluxes in the warm sector of the cyclone. This produced greater precipitation and lower static stability above the boundary layer, resulting in more rapid development. This observation is supported by Reed and Albright (1986) and Nuss and Kamikawa (1990), both of whom have noted the potential for positive heat fluxes northeast of the surface low to contribute to rapid cyclogenesis.

Nuss (1989) expanded upon Nuss and Anthes (1987) by explaining the relationship between surface fluxes and rapid development. He concluded that a pattern of heat and moisture fluxes, which results in an unstable planetary boundary layer (PBL) stratification northeast of the surface low and stable stratification in the warm sector, was most likely to lead to a vertical circulation resulting from PBL frictional convergence along the warm front. This in turn would carry latent heat above the boundary layer, warming the mid-troposphere, deepening and propagating the cyclone downstream.

Steeley (1990) used the planetary boundary layer model of Brown and Liu (1982) to calculate the surface fluxes in the region of the IOP-2 cyclone. His study of a single time period (0600 UTC 14 December) during the rapid development of the cyclone showed positive heat fluxes on the order of 100 $W m^{-2}$ south of the warm front. The study, however, gave no insight into the duration of the positive heat fluxes, nor their relative magnitude at other times.

Thus, the presence of strong heat fluxes to the east and northeast of the developing cyclone appear to be strongly linked to the rapid development of maritime cyclones. However, the length of time such fluxes persist (whether briefly or throughout the period of development) has not been fully determined.

C. AGEOSTROPHIC CIRCULATION AND FRONTAL CONVERGENCE

Upward heat fluxes require a source of cold, dry low θ_e air overlying relatively warm water. Nuss and Kamikawa (1990) demonstrated that the mechanism for providing a continuous supply of cold air to the baroclinic zone was the strong ageostrophic jet/frontal circulation that they observed in an explosive deepener that they studied off the east coast of Japan. The frontal circulation, which was the result of vertical forcing due to the superposition of divergence regions associated with two separate jet streaks, was observed as low-level easterly flow along the warm frontal zone. Kocin and

Uccellini (1985) have suggested that ageostrophic flows act to intensify the baroclinic zone, while surface heat fluxes (normally negative in the warm sector) act to reduce it. However, when fluxes in the warm sector are positive, as in the case of Nuss' (1989) sinusoidal SST gradient model, there is an accompanying decrease in static stability. This leads to an increase in downward momentum flux, frictional turning, and ageostrophic flow advecting cold air into the frontal zone. Nuss (1989) also notes that a cold air outbreak in the region northeast of the surface low is necessary to precondition the air in order to produce the upward heat and moisture fluxes he observed in his study. Such an outbreak could be the outflow from a downstream dying low pressure system to the east of the developing low - the Cold Conveyor Belt (Carlson, 1980). The relationship between PBL convergence and vertical circulation provides a necessary link between surface fluxes in the boundary layer and mid-tropospheric baroclinic processes.

The relationship between air-sea temperature differences and heat fluxes is well understood. Also, the presence of a low-level easterly flow has been observed in some actual rapidly-deepening cyclones. The degree to which this pattern of flow and surface heating characterizes other intense oceanic cyclones is not known.

D. VERTICAL AND SLANTWISE MOIST CONVECTION

Another aspect of vertical circulation that must be considered is that of moist symmetric instability, also called slantwise moist convection. It is well known that parcels that are vertically (buoyantly) unstable, or vertically neutral, in the presence of positive surface fluxes will be displaced upward until they reach hydrostatic equilibrium. This results in the release of latent heat and increased vorticity, which in turn leads to cyclogenesis. Moist symmetric neutrality is another stability condition which occurs in the atmosphere. M, the local approximation to absolute angular momentum, is given by

$$M = v_g + fx \tag{1}$$

and is conserved following parcels. f is the Coriolis parameter, x is the distance orthogonal to the thermal wind increasing towards warmer air, and v_g is the geostrophic velocity component parallel to the thermal wind (Emanuel, 1985 and Davis and Emanuel, 1988). Under conditions of moist symmetric neutrality, lines of constant θ_e and constant M will be parallel (that is, moist potential vorticity $q_e = 0$). When they cross such that θ_e isolines are more steep than M isolines, then moist symmetric insta-

bility exists ($q_e < 0$), and parcels will be displaced upward along the constant M surface, releasing latent heat.

The existence of moist symmetric instability is due to the fact that vertical wind shear, present in a frontal baroclinic zone, provides a source of energy in the form of centrifugal force in addition to the buoyant force. Thus, a parcel that is stable to vertical convection may be moist symmetrically neutral or unstable. This concept is particularly attractive because M surfaces are generally sloped in the same direction and magnitude as frontal surfaces, and because frontal zones are characterized by $q_e = 0$, an unlikely coincidence unless some form of slantwise moist convective adjustment is taking place (Davis and Emanuel, 1988). It should be noted that a parcel that appears to be moist symmetrically stable may be either absolutely stable or conditionally stable. The role of surface fluxes is implicated in the latter case, where low-level convergence as well as upper-level forcing could trigger the conditional instability.

Nuss and Kamikawa (1990) noted in their study of two similar coastal Japanese cyclones that the explosive cyclone featured areas of moist symmetric instability and increased boundary layer θ_e due to strong surface fluxes, while the non-deepener had moist symmetric neutrality and lower θ_e due to a less significant surface flux contribution. They suggested that the large surface heat and moisture fluxes in and to the north of the warm frontal baroclinic zone acted to destabilize the moist symmetric neutrality of the region. As a result, parcels in the frontal zone made a slantwise convective adjustment up the frontal slope (which approximates a constant M surface), releasing latent heat in the process. This results in an increase in the thickness of the 1000-500 mb layer, leading to increased vorticity advection in accordance with the Petterssen Development Equation (Petterssen, 1956). Emanuel (1988) has noted that imposed slantwise neutrality can double the growth rate of cyclones.

Under the conditions of slantwise neutrality in the vicinity of the frontal zone, surface heat and moisture fluxes will tend to destabilize the atmosphere, which leads to convection that contributes to the deepening and propagation of a developing cyclone. However, it is not yet known whether persistent fluxes in the warm frontal region are required to maintain that instability and to make a substantial contribution to development.

E. PERIOD OF MAXIMUM INFLUENCE OF SURFACE FLUXES

A final question concerns the period of greatest influence of the surface fluxes. Kuo et al. (1990) performed a series of 8 numerical experiments on 7 cases of explosive

deepening, in order to elucidate the role of surface energy fluxes both during and preceding rapid cyclogenesis. They discovered that fluxes occurring during the 24-h period of most rapid deepening had a negligible effect on that deepening. However, fluxes occurring during the 24 hours prior to rapid deepening had a significant effect. When fluxes were withheld from the 48-h runs, the cyclones weakened by an average of 7.1 mb at 24 h, and 13.5 mb at 48 h. Thus, fluxes occurring in the first 24-h period prior to rapid deepening have effects which are felt throughout the lifetime of the cyclone. A detailed examination of one representative western North Atlantic cyclone revealed that a region of upward energy flux existed in the early stages of cyclone development, resulting in a lowering of surface pressure over a large region in advance of the surface low. Furthermore, surface sensible heat flux associated with the Gulf Stream caused the formation of a coastal front which substantially increased low-level baroclinity, aiding cyclone development. As suggested by Nuss (1989), a previous cold outbreak left fresh polar air available to be conditioned by surface fluxes, thus reducing static stability within the PBL in the vicinity of the front. θ_e was found to have increased by as much as 37 K during the first 24-h period, much of it due to surface evaporation. The increased θ_e and reduced static stability both contributed strongly to heavy precipitation and latent heat release in the mid-troposphere ahead of the surface low, resulting in an added 11 mb of deepening during the 24-h period.

The implication in Kuo et al.'s (1990) study is that the 24-h period prior to the most significant cyclone development is critical to that development becoming explosive. It has not yet been demonstrated conclusively that fluxes in this period are always characteristic of rapid cyclogenesis.

F. OBJECTIVES

Numerous studies of explosively deepening maritime cyclones over the past few years following Sanders and Gyakum (1980) has greatly increased the understanding of these systems. However, many points still remain to be fully researched. The primary goal of this thesis is to examine the surface evolution and forcing as they occur in to the IOP-2 explosive cyclone. Specifically, the objectives can be stated as follows:

1. To examine for how long and during which stages of development the strong surface fluxes remain positive to the east and northeast of the developing IOP-2 cyclone, has been shown in numerical models (Nuss and Anthes, 1987 and Nuss, 1989) and in actual cyclones (Nuss and Kamikawa, 1990).
2. To determine whether strong low-level easterly flow is a characteristic of the IOP-2 cyclone as suggested by other explosively deepening cyclone studies.

3. To establish that the strong fluxes occur in the vicinity of the warm front, acting to maintain instability in the boundary layer.
4. To examine whether the fluxes exert a greater influence on cyclogenesis during the hours prior to rapid deepening, as Kuo et al. (1990) have found.

These questions will be examined during a discussion of the synoptic and mesoscale surface development of the IOP-2 cyclone in Chapter IV, and an analysis of the heat flux and thermal advection distributions in the cyclone in Chapter V.

III. DATA COLLECTION AND ANALYSIS METHODOLOGY

The primary objective of this research project was to determine the pattern of surface heat and moisture fluxes in the vicinity of a rapidly deepening maritime cyclone. Accomplishing this goal required a number of steps. They were:

1. Collecting raw data on surface pressure, temperature, dew point, winds, and sea surface temperature from a variety of sources.
2. Reducing the flight-level aircraft data to the surface.
3. Performing a detailed hand-analysis of the mean sea-level pressure (MSLP) and surface temperature fields in the vicinity of the IOP-2 cyclone for each 3-h time period.
4. Converting the hand analyses into a gridded numerical form of 20 km grid spacing using a Cressman analysis scheme.
5. Calculating surface fluxes from the gridded analyses using a modified Brown-Liu planetary boundary layer model.

A. DATA COLLECTION

The data collection effort for ERICA (Hadlock and Kreitzberg, 1988) was broad-based, utilizing a variety of unique sources developed specifically for the experiment, as well as many routinely available ones. A general breakdown of the number of surface data points gathered for each 3-h period, listed by data source, is provided in Table 1. Data were provided by specially-configured aircraft, both moored and drifting buoys, ships of opportunity and land-based surface observations. Fig. 1 shows the distribution of the ERICA buoy pattern, including existing moored buoys and initial deployment of drifting buoys.

The research aircraft flight level observations were the most significant sources of detailed data. They were flown into and throughout the region of the developing storm, allowing the positions of the low and the warm and cold fronts to be precisely located by wind shifts and strong temperature gradients. Most aircraft data points came from NOAA WP-3D aircraft, which were tasked with documenting the mesoscale structure of the low-level cyclone, frontal zones, updraft zones, and convection regions. The WP-3D's also deployed a new NCAR-developed dropwindsonde package (called a LeSonde); 17 of these were deployed in the study of IOP-2, 10 of which operated properly. The WP-3D's were also equipped with radar wind profilers. A similarly-equipped

Table 1. SUMMARY OF SURFACE DATA POINTS COLLECTED

Date/Time (UTC December 1988)	Ship and Buoy	Land	P3 Aircraft	Electra Aircraft	Total Data Points
13/1200	201	227		-	428
13/1500	103	234		-	374
13/1800	197	224		12	602
13/2100	87	230		117	435
14/0000	184	231	8	-	493
14/0300	91	202		1	355
14/0600	116	180	28	-	424
14/0900	82	179	-	-	261
14/1200	194	244	-	-	438

NCAR Electra also provided limited data from a region east of the cyclone center, in the region behind the warm front.

The meteorological buoy network consisted of several moored buoys, including four which were deployed near the center of the ERICA study area, and 37 air deployed drifting buoys. The goal was to achieve a buoy spacing of 200 km, with ship data supplementing the buoy data. The basic air-deployed buoy reports pressure, temperature, and sea-surface temperature (SST) through the ARGOS satellite every few hours, with the satellite determining the buoy's position within 500 m.

Ships of opportunity provided some useful information. Although the data suffered from uncertainty about the degree of error introduced by flow distortion around the ship, varying height above water of the readings, and human transcription errors, the same reporting units usually stayed in the same general area from one 3-h period to the next. Comparing the reports of individual units through successive 3-h periods gave a good idea of the relative change in temperature, pressure, and winds if not always a precise measurement.

Land-based surface observations were the most plentiful data sources, though the least useful for this study; they provided no direct indication of what was happening within the storm. However, they did facilitate reconstruction of the synoptic-scale picture of IOP-2.

Geostationary Operational Environmental Satellite (GOES) imagery, both IR and visible, was invaluable in the preparation of the mesoscale surface charts of the storm. Available at roughly one hour intervals, it provided excellent confirmation of the positions of the fronts and circulation centers. SST data was derived from NOAA Advanced Very High Resolution Radiometry (AVHRR) observations by National Environmental Satellite Data Information Service (NESDIS). The NESDIS Region 1 Regional-Scale SST analysis, covering a region from 52°W to 100°W longitude and from 5°N to 53°N latitude and with one-half degree (50 km) resolution, was interpolated down to a one-eighth degree (14 km) grid. The NESDIS Region 6 Local-Scale analysis, which covers the area from 60°W to 82°W longitude and 30°N to 46°N latitude at one-eighth degree resolution, was then substituted into the regional analysis. The entire region was then interpolated to a 20 km grid and combined with ship and buoy data using the Cressman analysis scheme to produce the analyses used in the air-sea interaction computations. The resulting SST analysis (Fig. 2) is presented for the period of the IOP-2 cyclone. It must be noted, however, that since the NOAA polar-orbiting satellite only retrieves SST data under clear conditions and only at 12 h intervals, the ages of the observations used in the analysis are variable. This can produce a "mosaic" effect in the analysis. The one-eighth degree local-scale analysis was performed at 0107 UTC 14 December 1988 using data that are up to 132 hours old. The one-half degree regional-scale analysis was performed at 0138 UTC 16 December 1988.

B. DATA REDUCTION

Aircraft data were taken continuously over a period of many hours for each IOP. In order to reduce the volume of aircraft data to a manageable quantity, the data was averaged over 30 s time intervals. Since this thesis is a study of the surface structure of a cyclone, it was necessary to reduce all flight level data to the surface in order to draft the hand-analyses of temperature and pressure. This was done by setting an arbitrary ceiling of 2000 m on the data being used, and disregarding all data taken above that level. However, the vast majority of the aircraft data used was taken at 350 m altitude, so the corrections were not severe in most cases. The temperature was reduced to the surface by assuming a moist adiabatic lapse rate,

$$\gamma_{average} \simeq 6.5°C\,km^{-1} \text{ where } \gamma = -\frac{\Delta T}{\Delta z}. \quad (2)$$

This may be assumed to hold true in the well-mixed boundary layer below 850 mb, since the entire area of interest is completely enshrouded by highly convective clouds.

Flight level pressure was reduced to the surface using the hypsometric equation, which is derived from the vertically integrated form of the hydrostatic equation

$$\frac{dp}{dz} = -\rho g. \tag{3}$$

The hypsometric equation relates the thickness of an atmospheric layer to two fixed constant pressure surfaces marking that layer's upper and lower bounds and is given by

$$\Delta Z = Z_2 - Z_1 = \frac{R_d \overline{T}_v}{g} \ln \frac{p_1}{p_2}, \tag{4}$$

where $\overline{T}_v$ is the mean virtual temperature of the layer, R_d is the specific gas constant for dry air, g is the acceleration of gravity, p_1 is the constant pressure at the lower level (the surface), p_2 is the constant pressure at the upper level (flight level), and ΔZ is the thickness of the layer in geometric meters (effectively the altitude of the aircraft). Observations originating from surface stations were accepted without modification.

There was some variation (approximately 1-2°C) between surface temperatures calculated from aircraft observations and those observed directly at the surface. This was presumably due to the fact that the actual atmospheric lapse rates were not always moist adiabatic. Aircraft temperatures were checked against surface temperatures at the same location wherever possible, and the mesoscale surface hand-analyses adjusted as necessary.

C. HAND-ANALYSIS OF DATA

The most time-consuming part of this thesis was the preparation of mesoscale hand-analyses of the IOP-2 storm from the raw surface data. Once all of the aircraft data had been reduced to the surface the data were divided into 3-h blocks, taking data from 90 minutes on either side of each time period (0000, 0300, etc). Each 3-h block of observations was then plotted on a large-scale map covering the entire IOP-2 development area (approximately 28°N to 45°N latitude and 55°W to 80°W longitude), and a regional analysis of surface temperature and pressure performed in intervals of 2°C and 4 mb. Next, a series of 3-h small-scale plots were prepared, each covering an area 14 degrees longitude by 7 degrees latitude and centered on the position of the IOP-2 low as it moved north and east. These were also analyzed, using contour intervals of 1°C and 2

mb of pressure, with the large scale analyses being used as a first approximation. Considerable time and effort went into making each 3-h analysis as consistent as possible with the previous time period's analysis and the available satellite imagery. The combination of GOES imagery and the large volume of observational data from the aircraft made it possible to place the low and the warm and cold fronts with a high degree of confidence.

D. CRESSMAN ANALYSIS OF IOP-2 DATA

In order to calculate the surface fluxes, it was necessary to convert the irregularly-spaced observational data into gridded data points using an objective analysis scheme. A Cressman (1959) analysis method was used, which consisted of making successive corrections to an initial guess. The initial guess used for the first time period analyzed (1200 UTC 13 December 1988) was the most recent NMC Spectral Grid Model (SGM) global analysis available. Subsequent time periods were analyzed using the previous time period's final analysis as a first-guess.

The analysis was to performed by making a series of five "scans", or passes through the data field, with each pass looking at increasing smaller scan radii around each grid point. Each grid square was 20 km on a side, and the dimensions of the analysis area were 111 by 53 grid units. The values for the scan radii used were 15, 11, 7, 4.5, and 2.25 grid units (300, 220, 140, 90, and 45 km), although this was sometimes varied depending on the amount of smoothing desired in the final product.

The result of this objective analysis scheme was two basic gridded surface level data fields for each 3-h time period - temperature and mean sea level pressure (MSLP). Due to the lack of dewpoint observations and an adequate method of reducing aircraft winds to the surface, these fields were not used in this study, as they contain substantial errors. A computer-generated contoured analysis from each gridded data set was prepared, and compared with its companion hand-analysis for the same time period. The gridded analysis was then modified by the addition of bogus data points and the deletion of obviously erroneous or inconsistent data points in order to force the Cressman analysis to resemble the hand-analysis in its major features, such as the location and depth of the low and the regions of significant thermal advection.

E. FLUX CALCULATIONS IN PLANETARY BOUNDARY LAYER

The final step in the determination of the sensible and latent heat fluxes associated with IOP-2 was to pass all the available data fields (SST, surface air temperature, and

estimated relative humidity) to the large-scale marine planetary boundary layer (PBL) model developed by Brown and Liu (1982).

The model is basically a two-layer model which relates surface stress (τ_0) to geostrophic flow (G) over a flat surface. The flat surface in this model has been modified to account for surface roughness (z_0) due to wave generation and humidity effects. Synoptic-scale pressure fields are used to calculate geostrophic flow, which is corrected for gradient wind effects, and serves as the upper boundary condition. Stratification effects within the boundary layer are determined from air-sea temperature differences, and synoptic-scale temperature fields allow thermal wind effects to be calculated.

This two-layer model deals with the surface layer and the Ekman/Taylor layer above it. The surface layer has a logarithmic profile wherein the surface stress is assumed to be constant in the lowest several meters of the atmosphere. This relationship is given by

$$\frac{u}{u_*} = \frac{1}{k}\left[\ln\left(\frac{z}{z_0}\right) - \psi\left(\frac{z}{L}\right)\right], \tag{5}$$

where u_* is the friction velocity, z_0 is a roughness length chosen such that $u = 0$ at $z = z_0$, k is von Karman's constant, and the similarity function ψ is a function of the stability parameter z/L. The Obukhov length L is a scaling parameter that is useful in the surface layer.

The upper layer of the Brown-Liu PBL model is an Ekman/Taylor layer, a region in which turbulent eddies tend to be nearly constant with height. It is within this layer that thermal wind effects are calculated. The result is a thermal wind-modified 'Ekman Spiral', which describes the departure of the winds from geostrophic balance within the boundary layer. At the top of this layer, which is typically 1 km high, the wind is parallel to the geostrophic wind. This level is designated as the top of the PBL (also called the gradient wind level).

To determine the Obukhov length for this marine PBL model, that surface latent and sensible heat fluxes must be calculated. One interpretation of the Obukhov length (Stull, 1988) is that it is proportional to the height above the surface at which buoyant factors first dominate over mechanical (shear) production of turbulence. In general, $L > 0$ implies stable air, and $L < 0$ implies instability in the surface layer. The Obukhov length is given by

$$L = \frac{\rho_a u_*^3}{k\overline{w'\rho'}g} = -\frac{\rho_a u_*^3}{kB}. \tag{6}$$

B is the buoyancy flux, where

$$B = -\overline{w'\rho'}g = \rho_a \frac{\overline{w'T'_v}g}{\overline{T}_v}. \tag{7}$$

B can be expressed in terms of latent ($\tilde{Q}_E$) and sensible ($\tilde{Q}_H$) heat fluxes as follows:

$$B = \frac{\rho_a g}{\overline{T}_v}[\overline{w'T'} + 0.61\overline{T}\,\overline{w'q'}] \tag{8}$$

$$B = \frac{\rho_a g}{\overline{T}_v}[\frac{\tilde{Q}_H}{\rho_a C_{pa}} + 0.61\overline{T}\frac{\tilde{Q}_E}{\rho_a L_v}], \tag{9}$$

where $\overline{w'T'}$, $\overline{w'q'}$, and $\overline{w'\rho'}$ are the vertical turbulent heat, moisture, and buoyancy fluxes, respectively, and $\overline{T}$ and $\overline{T}_v$ are the mean and mean virtual temperatures in the layer. The density of the atmosphere in the boundary layer ρ_a is assumed tc be constant by the Boussinesq approximation. C_{pa} is the specific heat of air under constant pressure.

The relationship which is used to calculate the sensible heat flux $\tilde{Q}_H$ is given by

$$\tilde{Q}_H = \rho_a C_{pa}\overline{w'T'}. \tag{10}$$

However, the value of the specific heat for air, C_{pa}, varies with humidity approximately as

$$C_{pa} = C_{pd}(1 + 0.84q) \quad \text{where} \quad \{[C_{p\,\text{water vapor}} - C_{pd}]/C_{pd}\} = 0.84. \tag{11}$$

Combining the two equations above yields

$$\tilde{Q}_H \simeq \rho_a C_{pd}(\overline{w'T'} + 0.84\overline{T}\,\overline{w'q'}). \tag{12}$$

The last term in the above equation accounts for approximately a 10% change in the estimate of sensible heat flux as compared to using only the dry specific heat, and so is an important factor in the marine environment. The corresponding expression for latent heat flux is

$$\tilde{Q}_E = \rho_a L_v \overline{w'q'}. \tag{13}$$

The above relationships show the contribution of latent and sensible heat flux to buoyancy flux. It is observed over the ocean that $\tilde{Q}_E$ typically has a value 10 times larger than $\tilde{Q}_H$. However, the terms $\tilde{Q}_H/\rho_a C_{pa}$ and $0.61\overline{T}\tilde{Q}_E/\rho_a L$, are both of the same order of magnitude, and thus both must be considered. If both $\tilde{Q}_E$ and $\tilde{Q}_H$ are positive, then $L < 0$. There is a net upward heat flux, and the air is unstable. If both are negative, then $L > 0$. The heat flux is downward, and the air is stable. The model calculates these surface fluxes through an iterative scheme, where the gradient wind is used as a first-guess to get the friction velocity u_*. The resultant fluxes then provide a more accurate measure of the Obukhov length from which a new surface wind (friction velocity) is calculated. This process is repeated until the surface wind converges to a constant value For highly unstable conditions (weak winds and strong horizontal temperature gradients) convergence does not always result and incorrect fluxes and winds are output.

Several adjustments to the basic data sets had to be made prior to passing them to the Brown-Liu model, which is applied at each grid point independently. First, the relative humidity fields resulting from the Cressman analysis were not used as noted above. Instead, a constant relative humidity of 70% was assumed throughout the area of study. This may have been too high in some areas, and too low in others, but it was a reasonable average over the entire area, given the amount of convective activity and rainfall.

When the surface pressure from the Cressman analysis was passed to the PBL model, it was smoothed five times prior to being used for PBL calculations in order to reduce the number and severity of the unrealistically tight pressure gradients and the resulting strong geostrophic winds. The geostrophic winds were then calculated from the smoothed pressure fields, then curvature effects added to get the gradient level winds. The PBL winds finally were calculated by determining the frictional turning resulting from eddy viscosity K in the Ekman layer. The heat fluxes are a numerical byproduct of the PBL wind calculations, and are easily plotted once the PBL winds have been generated. The resulting heat and moisture fluxes, and their physical interpretation are presented in Chapter V.

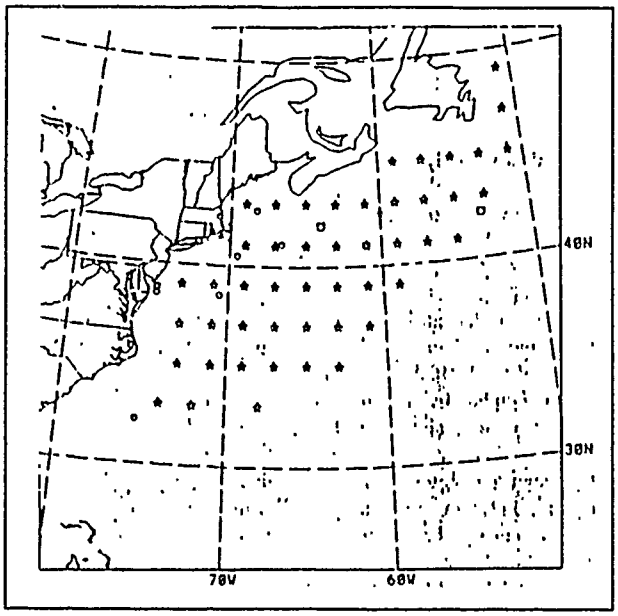

Fig. 1. Map of ERICA buoy pattern: Stars mark the points of deployment of the initial array of 48 drifting buoys (approximately 200 km spacing). Circles mark the existing deepwater moored buoys, primarily in coastal waters. Four deep-water moored buoys are indicated by squares (Hadlock and Kreitzberg, 1988).

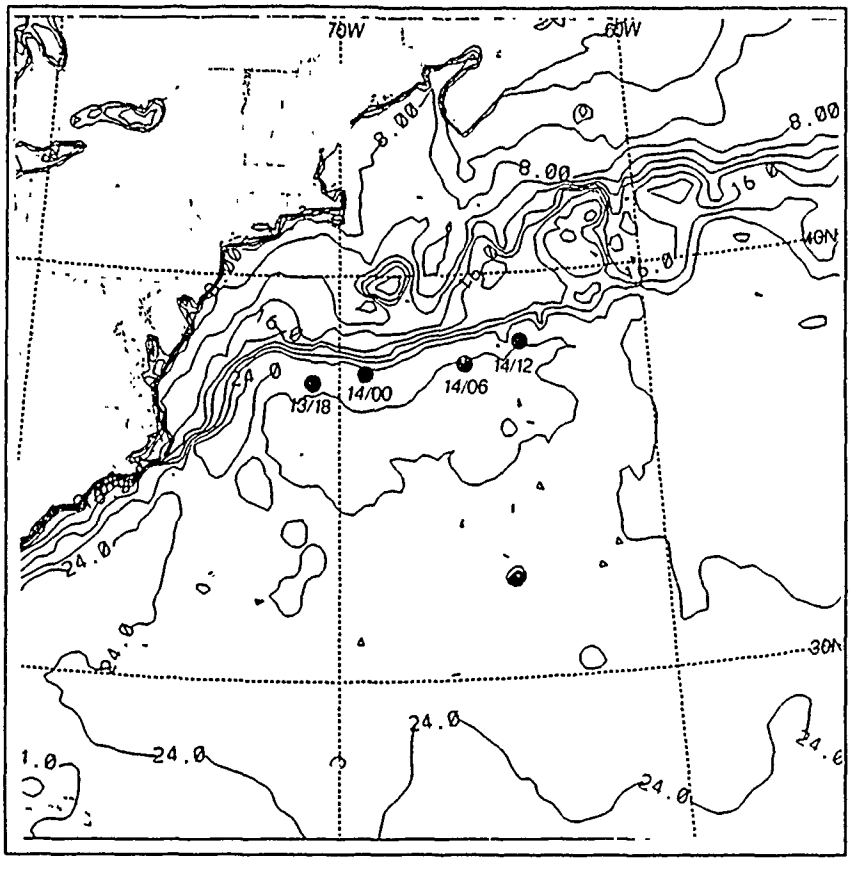

Fig. 2. **SST Analysis for 14-16 December 1988:** Sea-surface temperature based on NOAA AVHRR data, in 2°C contours. Track of IOP-2 cyclone is marked at 6 h intervals.

IV. SYNOPTIC DISCUSSION OF IOP-2

Chalfant (1989) has given a detailed description of the dynamical development of the IOP-2 cyclone. She noted that the storm began as a low off the east coast of Florida, which formed in response to forcing by a 500 mb shortwave trough. After a brief period of rapid deepening, this "early" low continued to develop at only a modest rate following the passage of the upper-level trough. The arrival 12 h later of a second and stronger 500 mb shortwave trough over the coast caused the formation of two more lows, one of which deepened explosively - the "IOP-2 low". It experienced a central pressure fall of 30 mb in one 12-h period, dropping to 968 mb by the end of the period of rapid development.

In his analysis of IOP-2 surface fluxes, Steeley (1990) noted that the northern (IOP-2) low developed in a region characterized by a weak thermal gradient and weak warm air advection east of the low. He also noted that the low followed the south boundary of the Gulf Stream, a region of strong sea-surface temperature (SST) gradient (Fig. 2 on page 19). Working with mean sea-level temperature and isotherm analyses based on the data then available, Steeley (1990) used the PBL model of Brown and Liu (1982) on a preliminary version of the IOP-2 surface analysis to determined that maximum warming at 0600 UTC 14 December occurred east and northeast of the northern (IOP-2) low. Based on the correspondence between the largest surface heat fluxes and the largest warming, Steeley (1990) suggests that the warming was due more to surface fluxes than to warm advection.

Using the previous work of Chalfant (1989) and Steeley (1990), plus surface analyses done by Sanders (1989) as a guide, the mesoscale surface structure of the IOP-2 low was reconstructed and the surface fluxes calculated, as described in Chapter III. The chronology of the development of the IOP-2 cyclone, which includes the results of the mesoscale analysis of the storm, is detailed below. The results of the surface flux calculations will be presented in Chapter V.

A. 0000 - 1200 UTC 13 DECEMBER 1988

As Chalfant (1989) pointed out, the central event of this time period is the appearance of two upper-level shortwave troughs, which forces the development of two surface lows. The first trough, which is seen in the 0000 UTC 13 December (hereafter, date and time will be denoted by day/time UTC, e.g., 13/0000 UTC) NOGAPS (Naval Opera-

tional Global Atmospheric Prediction System) 500 mb analysis (Fig. 3), lies over the Carolinas and Georgia, and features height falls of 10-50 m. This trough initiates the first low pressure center off the east coast of Florida. By 13/1200 UTC this southerly low has migrated from its area of formation to a point off the coast of Florida (28°N, 70°W) and has deepened to 1004 mb. It is visible in the 13/1231 UTC GOES IR imagery (Fig. 4) as a cloud band extending southwest to northeast, with the centers of maximum convection occurring at the low and along the warm front. GOES visible imagery for 13/1231 UTC (Fig. 5) clearly shows a narrow line of convective activity extending from the vicinity of the Florida Keys, marking the cold front, and then broadening out to join the low pressure center and continuing northeast as the warm front. The broad region of deep convective activity to the northeast of the surface low pressure system is associated with the upper-level vorticity advection maximum of this first shortwave moving rapidly to the east.

The second shortwave trough on the 13/0000 UTC 500 mb analysis (Fig. 3) is located over Michigan and Wisconsin, and features height falls of 100 m, which increase to 150-160 m in the later part of this period. This trough is associated with the incipient IOP-2 low, which is visible in the 13/1231 UTC GOES IR image (Fig. 4) as only a loosely organized mass of mid-level clouds off Cape Hatteras. The 13/1200 UTC mesoscale analysis of isotherms and sea-level pressure (Fig. 6) shows the IOP-2 trough beginning to develop as an inverted surface trough located on the north side of the earlier low pressure system. The mesoscale analyses depict the surface thermal and pressure contours based on all available data. For clarity, only a few representative data points are included in the drawings. Wind observations reveal that the surface air flow east of the incipient IOP-2 low is easterly, and that the wind direction is essentially parallel to the isotherms. In some areas there is weak cold advection in that region.

Another significant feature is a strong high developing approximately 700 nm northeast of the IOP-2 low. It has intensified to 1027 mb, and is clearly visible as the clear area between Maine and the southerly low's cloud shield. This high is a source of cold air at the surface as it acts together with an old and filling 992 mb low southeast of Greenland (visible in the vicinity of 40°N, 40°W) to channel cold, low level outflow into the region ahead of the IOP-2 low. The primary low-level baroclinic zone east of the low is displaced to the south of the Gulf Stream ($\sim 38°N$), as a result of this cold northeasterly flow to the east of the IOP-2 cyclone.

B. 1500 - 1800 13 DECEMBER 1988

The 13/1500 UTC mesoscale analysis (Fig. 7) shows that the IOP-2 low has deepened to 1007 mb. This probably coincides with the arrival of the PVA region ahead of the stronger and more northerly of the two upper-level troughs over the central North Atlantic coast. The baroclinic zone east of the low which was south of the Gulf Stream at 13/1200 UTC has shifted northward to approximately coincide with the Gulf Stream. This rapid shift of the baroclinic zone is associated with very rapid warming of the cold air to the south of the Gulf Stream. Several buoys warm by 2-3°C in the 3-h period, although there continues to be a large (5-10°C) temperature difference between the SST and the overlying air. For example, buoy 362E at 38°N, 63°W warmed by 2.8°C in the period 13/1200 - 13/1500 UTC. Mesoscale frontal analysis for 13/1800 UTC (Fig. 8; note the northward frame shift of the analysis) shows that a distinct frontal wave has formed, and that the warm front is aligned along the south boundary of the Gulf Stream, as is the low itself. The low has deepened to 1002 mb. During the 6 h from 1200 to 1800 UTC the IOP-2 low has deepened by 7 mb, which represents a deepening rate of 1.7 Bergerons (B) when normalized to 24 h. The positions of both fronts are well-established by low-level aircraft observations at this analysis time.

For the first time, evidence of some warm advection northeast of the IOP-2 low is present in the cold air to the north of the warm front. The flow remains basically parallel to the isotherms to the south of the front, which indicates that little or no advection is taking place at the surface in the warm sector.

The southerly low, by contrast, has deepened by only 4 mb, to 1000 mb, and is migrating southeast. The cyclonic flow pattern for this low as seen in Sanders' (1989) regional isotherm and sea-level pressure analysis for 13/1800 UTC (Fig. 9) produces easterly flow to the north of the southerly low. This blocks what would have been typical warm air advection in a southerly flow. This flow pattern results in a broad region of low-level easterly flow, which may become substantially warmed and moistened by the relatively warm sea surface.

The high to the northeast continues to build, and has reached a central pressure of 1029 mb by the end of this period. Its anticyclonic flow helps to direct cold air from the northeast southward towards the developing cyclone center.

C. 2100 UTC 13 DECEMBER - 0000 UTC 14 DECEMBER 1988

Mesoscale analysis for 13/2100 UTC (Fig. 10) shows that the IOP-2 low has deepened to 998 mb and moved very slowly eastward, roughly parallel to the south

boundary of the Gulf Stream. The warm front is analyzed from the convergence in the aircraft winds at 66.6°N, 36.5°W and lies in the middle of equally strong temperature gradients to the north and south of the front. The strongest temperature gradients along the cold front are in the cold sector.

The 14/0000 UTC mesoscale analysis (Fig. 11) shows the development of two surface baroclinic zones behind the cold front as the cyclone continues to propagate east. One represents the baroclinity associated with the surface cold front and the other occurs at approximately the position of the Gulf Stream as it extends to the south. Note the weak temperature gradient between observations at 34.9°N, 72.9°W and 34.5°N, 70.4°W. The low, now positioned at 37.3°N, 69.8°W, is centered directly under the large cloud shield which is clearly seen in the GOES IR imagery for 14/0031 UTC (Fig. 12). The cold front extends out from under the dense multi-layered clouds as a band of low and mid-level clouds passing through 30°N, 72°W. The southerly low is clearly visible as a large comma-shaped cloud at 35°N, 60°W. During this 6 h period the IOP-2 low deepened to 996 mb, a 2.1 B rate normalized to 24 h.

The southerly low continues to deepen slowly, reaching a central pressure of 996 mb, although operational 500 mb analyses show that it no longer has any upper-level support. Sanders' (1989) analysis for 14/0000 UTC (Fig. 13) shows that the strong anticyclone northeast of the IOP-2 low and the southerly low combine to produce southeasterly flow to the east of the IOP-2 low.

As noted by Steeley (1990), the most dramatic surface warming is seen in the vicinity of 40°N, 68°W, northeast of the IOP-2 low, where temperatures have risen as much as 5°C ahead of the low during this 12-h period ending at 13/1800 UTC. The next chapter will examine the factors which contribute to this large surface temperature increase.

D. 0300 - 0600 UTC 14 DECEMBER 1988

This is the period during which the most rapid deepening of the IOP-2 cyclone occurs. The 14/0300 UTC mesoscale analysis (Fig. 14) shows that the IOP-2 low has become well-organized, has deepened to 989 mb, and that the thermal gradient is well-aligned along the warm front, with the strongest gradient north of the front. Also, the cold front in the vicinity of the low appears to have moved east, ahead of the strongest thermal gradient. This structure closely resembles the "frontal fracture" of the Shapiro and Keyser (1990) model of extratropical cyclogenesis. It is significant that development is continuing despite the fact that the storm seems to be moving away from

the strongest surface baroclinic structure. The low center continues to move easterly as it develops and deepens.

GOES IR imagery for 14/0601 UTC (Fig. 15) shows that the comma head of the IOP-2 low is a large, well-defined area of cold cloud tops. Mesoscale analysis for 14/0600 UTC (Fig. 16) shows that the trends of the previous 3 h have continued. The "frontal fracture" of the cold front has increased as the midsection of the front bends eastward away from its supporting baroclinic structure. It is well-defined by surface observations on both sides of the cold front at this time. The cyclone has deepened 12 mb in 3 h to 977 mb, a normalized deepening rate of 5.7 B. It is evident in Fig. 15 that the strongest surface baroclinity is located north of the warm front and parallel to the SST gradients associated with the continental shelf. This baroclinic feature will be referred to as the Continental Shelf Break Front. The cyclone is beginning to occlude as the cold front is moving rapidly eastward.

The southerly low has moved east-southeasterly, and deepened only slightly, to 992 mb. The poor organization of the system in the satellite imagery emphasizes its weakness. GOES IR imagery for 14/0601 UTC (Fig. 15) shows the IOP-2 cloud shield dominating the western Atlantic. The southerly low's cloud mass, by comparison, is now only loosely organized, and has in fact lost a considerable amount of its vertical development, as seen by the diminishment in the extent of the number of cold cloud tops along the cold front. With the surface low and moisture situated in the southeasterly flow around the IOP-2 cyclone, the southerly low is being rapidly drawn into that cyclone, and will eventually be absorbed.

E. 0900 - 1200 UTC 14 DECEMBER 1988

GOES IR imagery for 14/1231 UTC (Fig. 17) shows that the entire western Atlantic is dominated by the fully-developed comma cloud pattern associated with the IOP-2 cyclone centered on 38.3°N, 64.4°W. The previously distinct southern low has been completely integrated into the storm. Visible imagery for 14/1231 UTC (Fig. 18) shows a broadly developed cloud shield over the entire area. Central pressure has dropped to 968 mb at 1200 UTC, which is a 9 mb drop in this 6-h period and a 1.6 B normalized drop. Mesoscale analysis for 14/0900 UTC (Fig. 19) shows that the fronts have become almost completely occluded, resembling the "T-bone" structure of Shapiro and Keyser (1990). The thermal gradients, which have been drawn to be consistent with the previous time periods' analysis which were based on surface observations in the vicinity of the low, have weakened substantially. These facts clearly indicate that the period of rapid

deepening is over. After 14/1200 UTC, the storm weakens slowly and fills as it moves northeastward.

F. SUMMARY OF DEVELOPMENT

The following summarizes the principal points of the development of ERICA IOP-2. The storm first began with a "preliminary" low off the coast of Florida, which was generated by the passage of a short-wave upper-level trough early on 13 December 1988. This first low migrated northeast and continued to deepen, but not explosively, as the first trough passed east of the low. A second and much stronger shortwave trough passed over the coast later on 14 December, causing the development of a second low slightly northwest of the first low. This second low - the IOP-2 low - had a number of special attributes:

- The IOP-2 developed in the vicinity of strong sea-surface temperature gradients associated with the Gulf Stream.
- The IOP-2 low was supported by strong upper-level vorticity advection throughout its period of most intense deepening.
- Warm thermal advection at the surface by the IOP-2 low's cyclonic circulation pattern was inhibited by the presence to the southeast of the preliminary low formed by the passage of the first upper-level trough.
- Low-level cold outflow from an old and filling cyclone in the mid North Atlantic produced a pool of cold air at the surface in advance of the storm's path.
- The region east and northeast of the IOP-2 low experienced rapid surface temperature increases, on the order of 5°C in the 6 h prior to the period of most rapid development.

The 6-h period between 0000 and 0600 UTC 14 December 1988 was the period of explosive development, with the storm deepening by 19 mb during that time. The chronology of the storm's development central pressure and movement of the low is summarized in Table 2. The overall development rate of the storm is 2.34 B, for a pressure drop of 40 mb in the 24 h of most rapid development. The evidence of the presence of cold outflow, lack of strong warm advection ahead of the storm at the surface, and rapid surface temperature rises seem to clearly imply a role for surface fluxes in the explosive development of the IOP-2 cyclone. The next chapter will present an analysis of surface heat and moisture fluxes in IOP-2 to quantify the degree to which the surface fluxes warmed and moistened the air in advance of the IOP-2 cyclone.

Table 2. SUMMARY OF DEVELOPMENT OF IOP-2

Date/Time (UTC December 1988)	Surface Position (Lat/Long)	Central Pressure (mb)	3-h Deepening Rate (Bergerons)
13/1500	36.0°N/73.0°W	1007	1.92
13/1800	37.5°N/71.0°W	1002	2.40
13/2100	37.6°N/71.4°W	998	2.88
14/0000	37.7°N/69.8°W	996	0.96
14/0300	38.2°N/68.0°W	989	3.36
14/0600	37.6°N/66.3°W	977	5.68
14/0900	37.8°N/64.4°W	972	1.42
14/1200	38.3°N/64.4°W	968	1.89

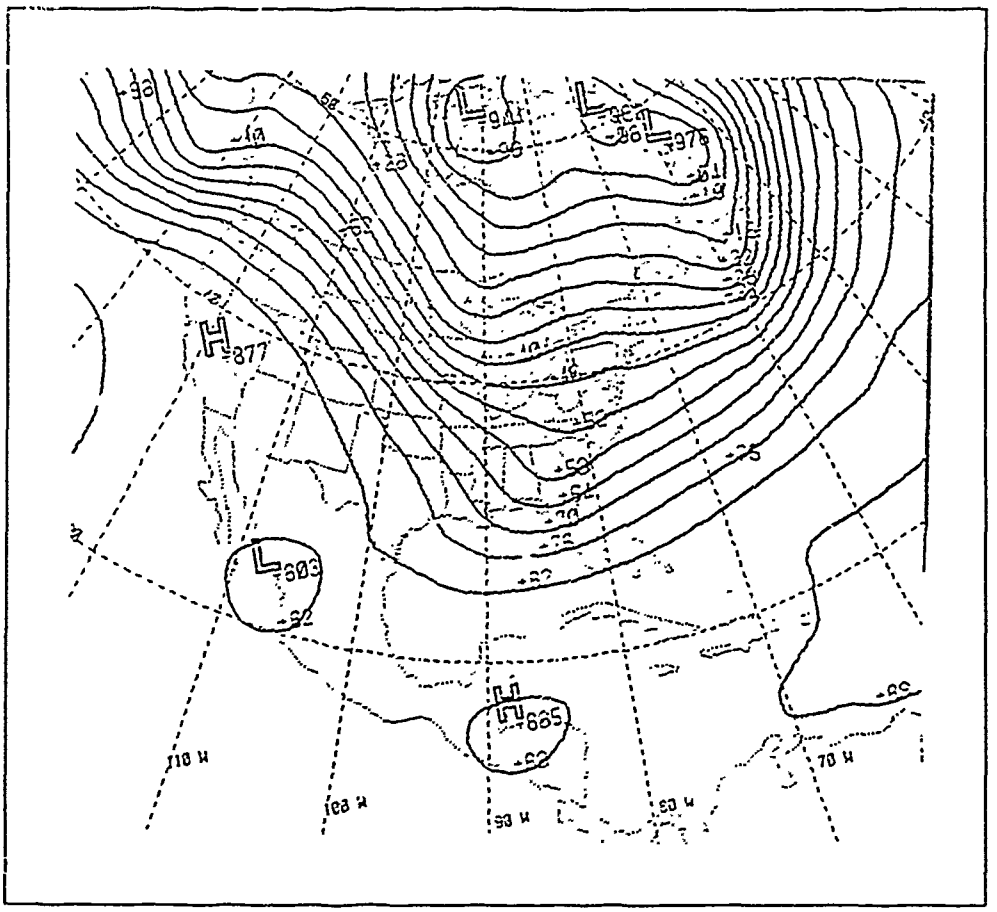

Fig. 3. FNOC NOGAPS Analysis for 13/0000 UTC December 1988:

Fig. 4. GOES IR imagery for 13/1231 UTC December 1988: U.S. East Coast sector.

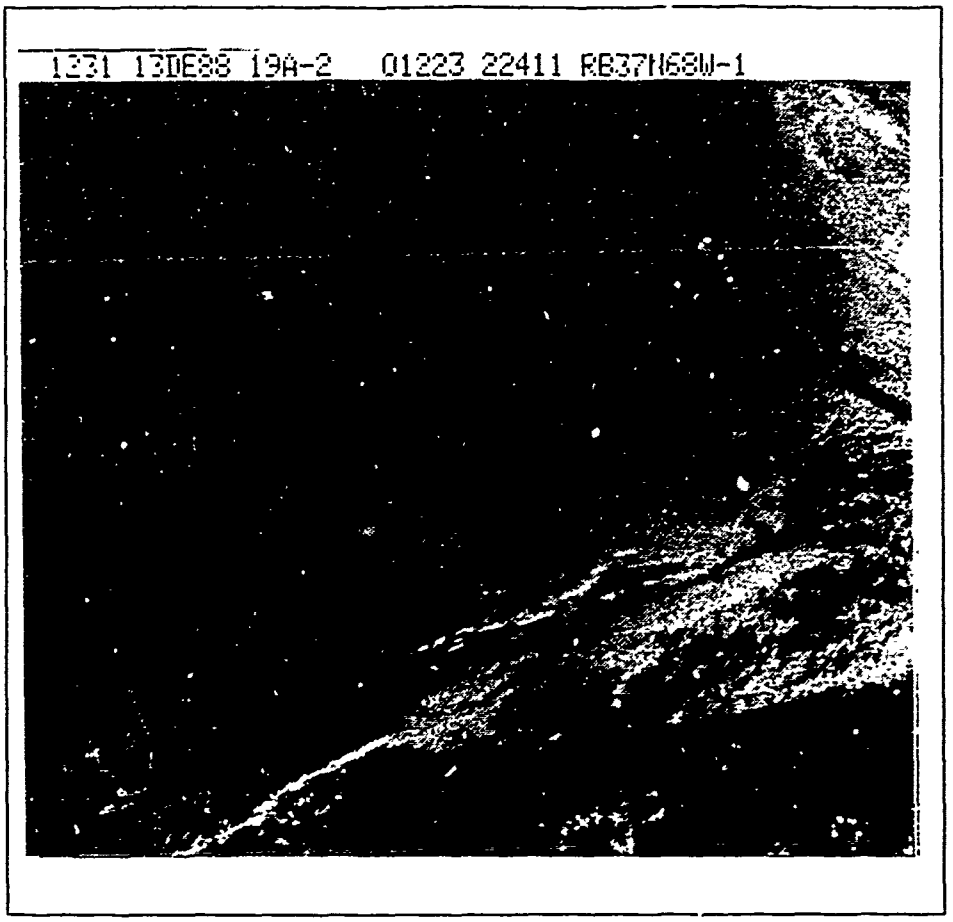

Fig. 5. GOES VIS imagery for 13/1231 UTC December 1988: U.S. East Coast sector.

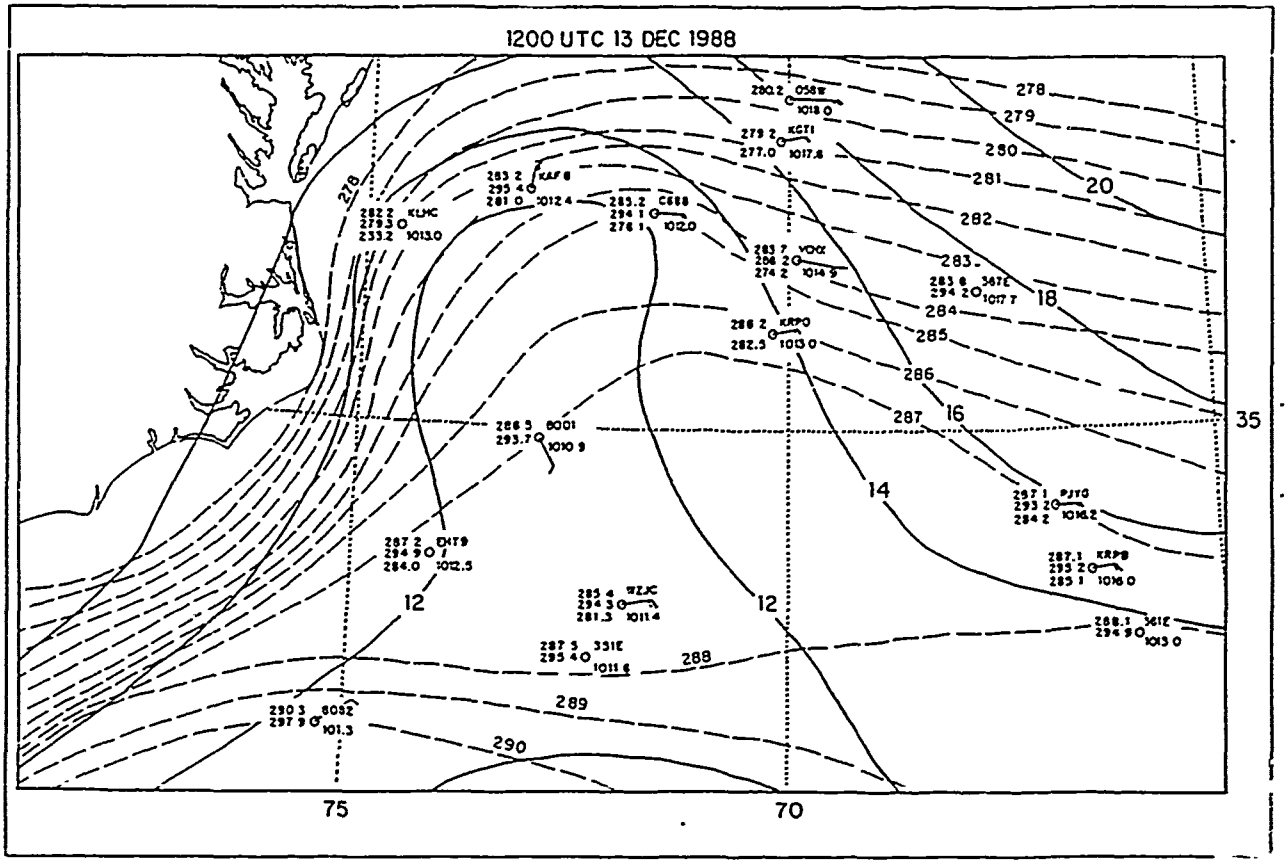

Fig. 6. IOP-2 13/1200 UTC December 1988 mesoscale surface frontal analysis: Sea-level pressure (solid) in mb and surface temperature (dashed) in °C.

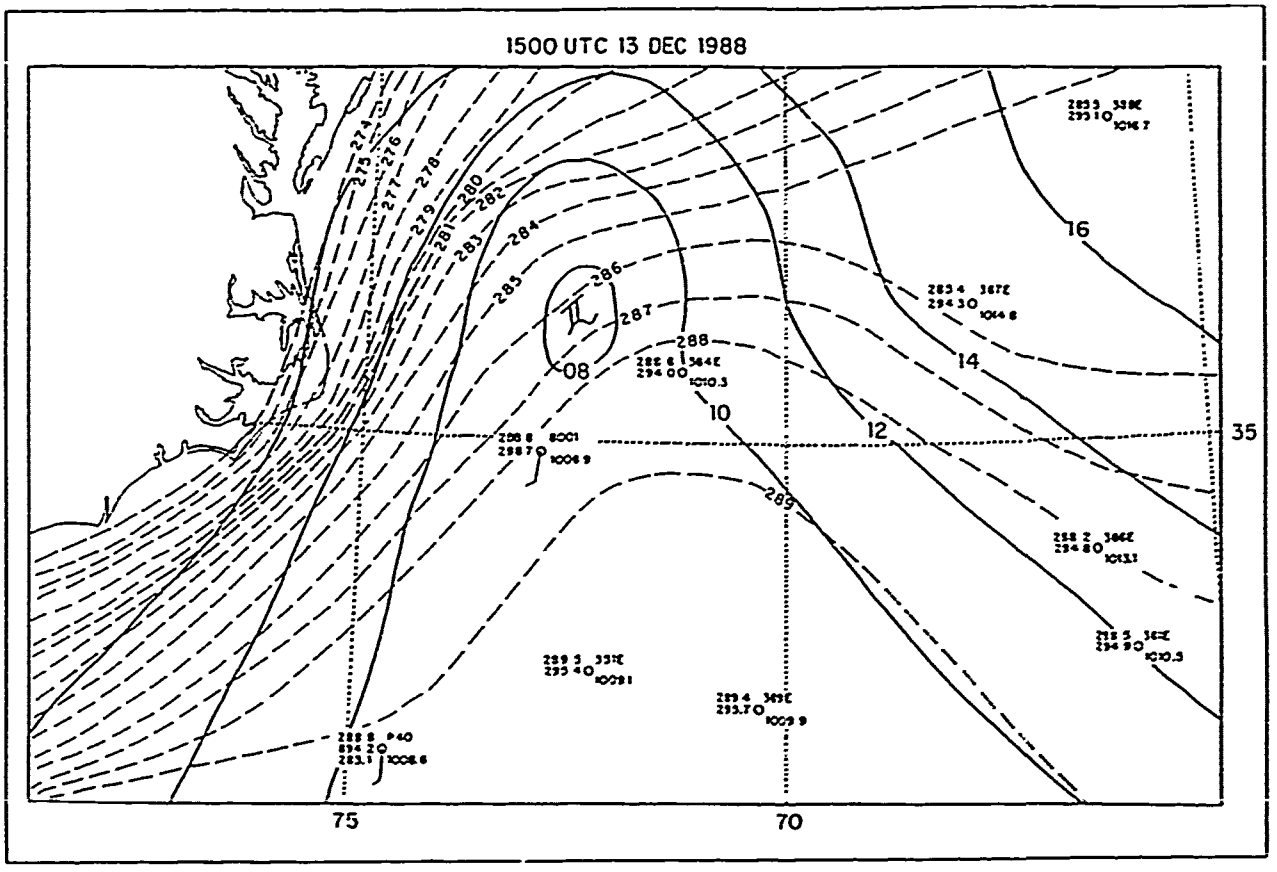

Fig. 7. IOP-2 13/1500 UTC December 1988 mesoscale surface frontal analysis: Sea-level pressure (solid) in mb and surface temperature (dashed) in °C.

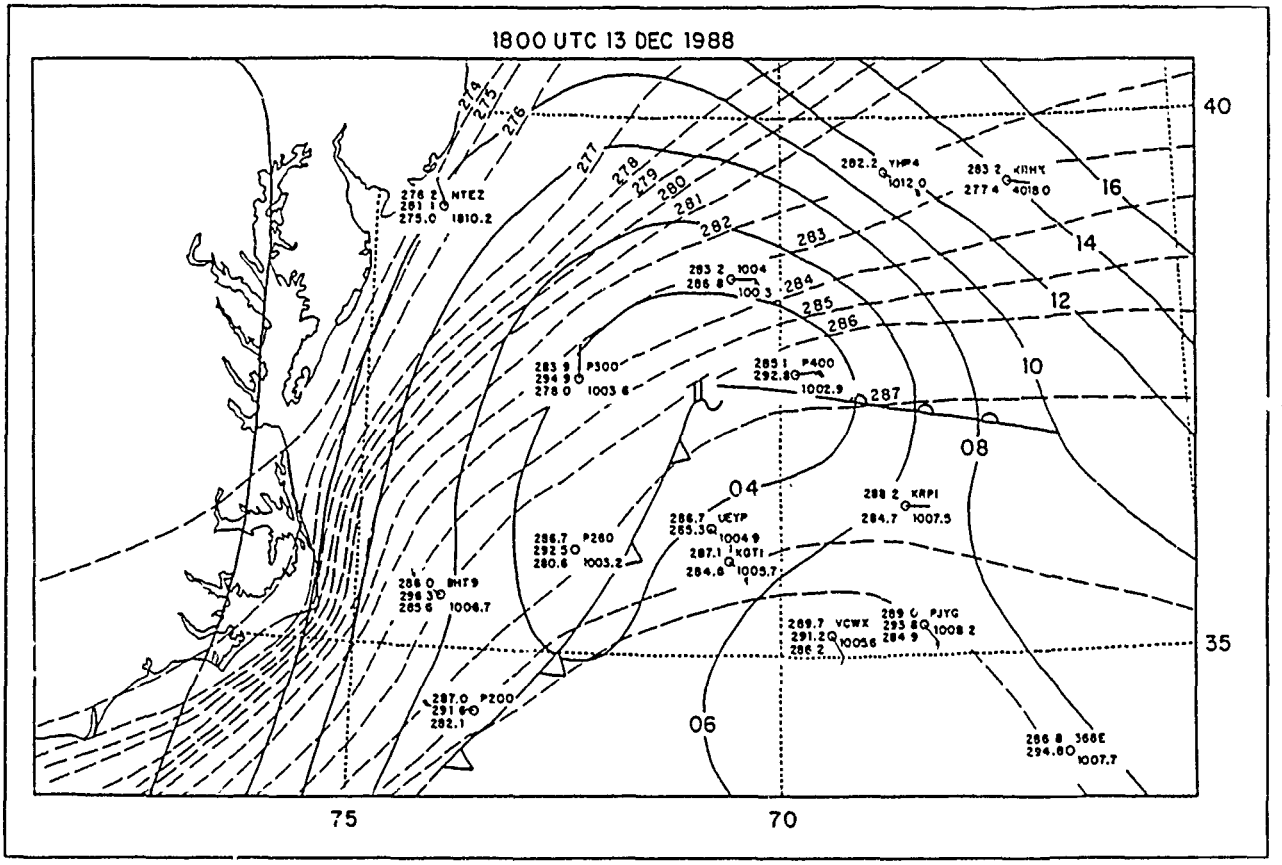

Fig. 8. IOP-2 13/1800 UTC December 1988 mesoscale surface frontal analysis: Sea-level pressure (solid) in mb and surface temperature (dashed) in °C.

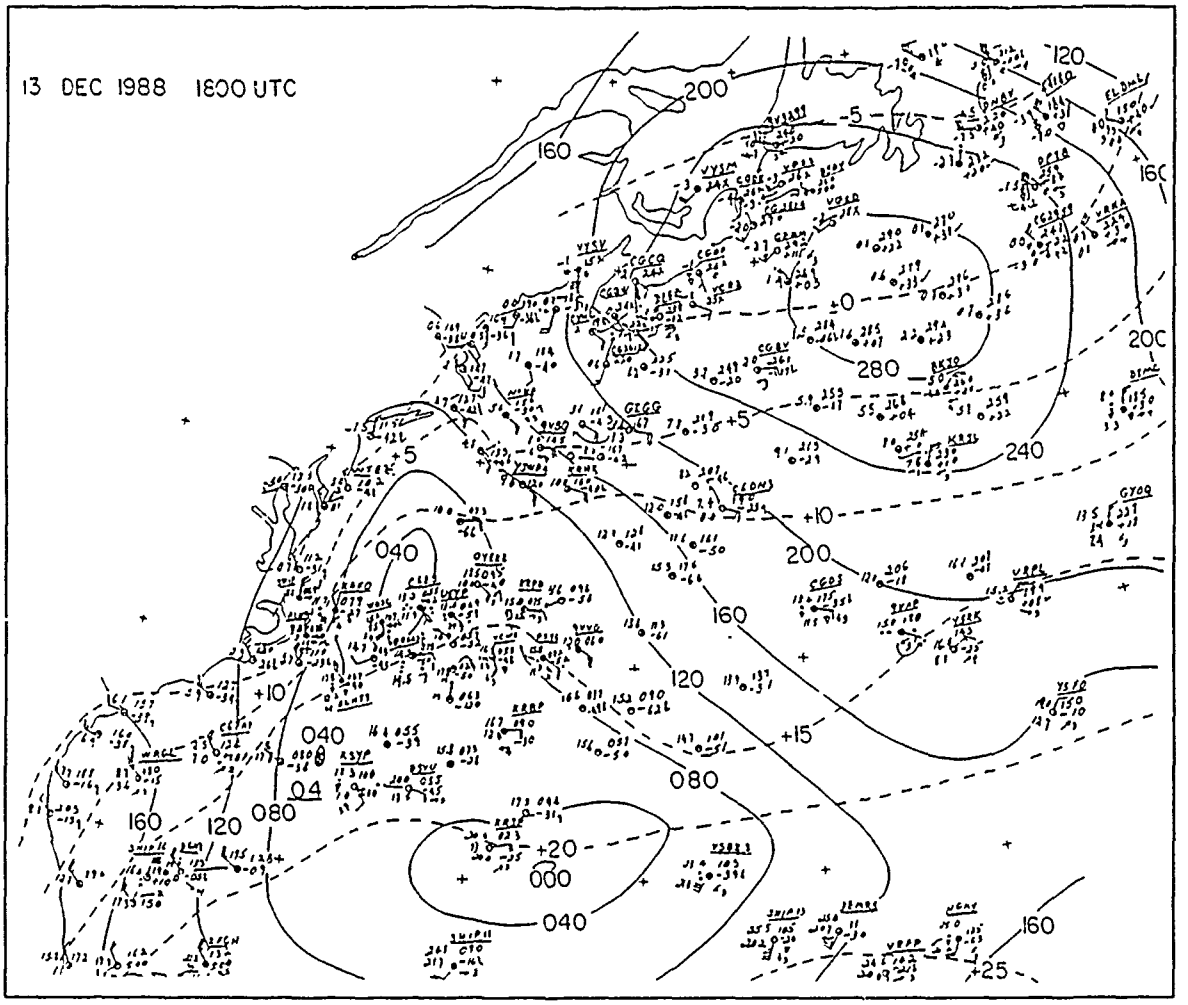

Fig. 9. IOP-2 13/1800 UTC December 1988 surface analysis: Sea-level pressure (solid) in tenths of mb where the leading 9 or 10 has been dropped and surface temperature (dashed) in °C (Sanders, 1989).

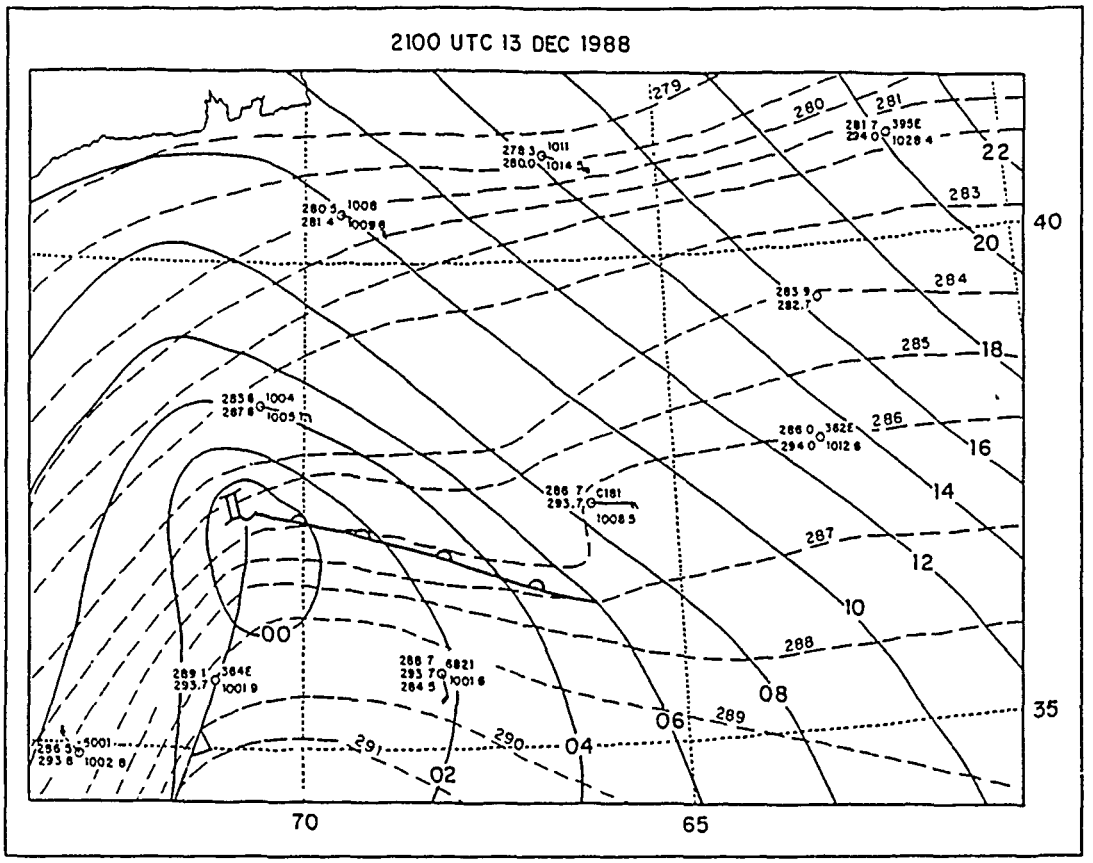

Fig. 10. IOP-2 13/2100 UTC December 1988 mesoscale surface frontal analysis: Sea-level pressure (solid) in mb and surface temperature (dashed) in °C.

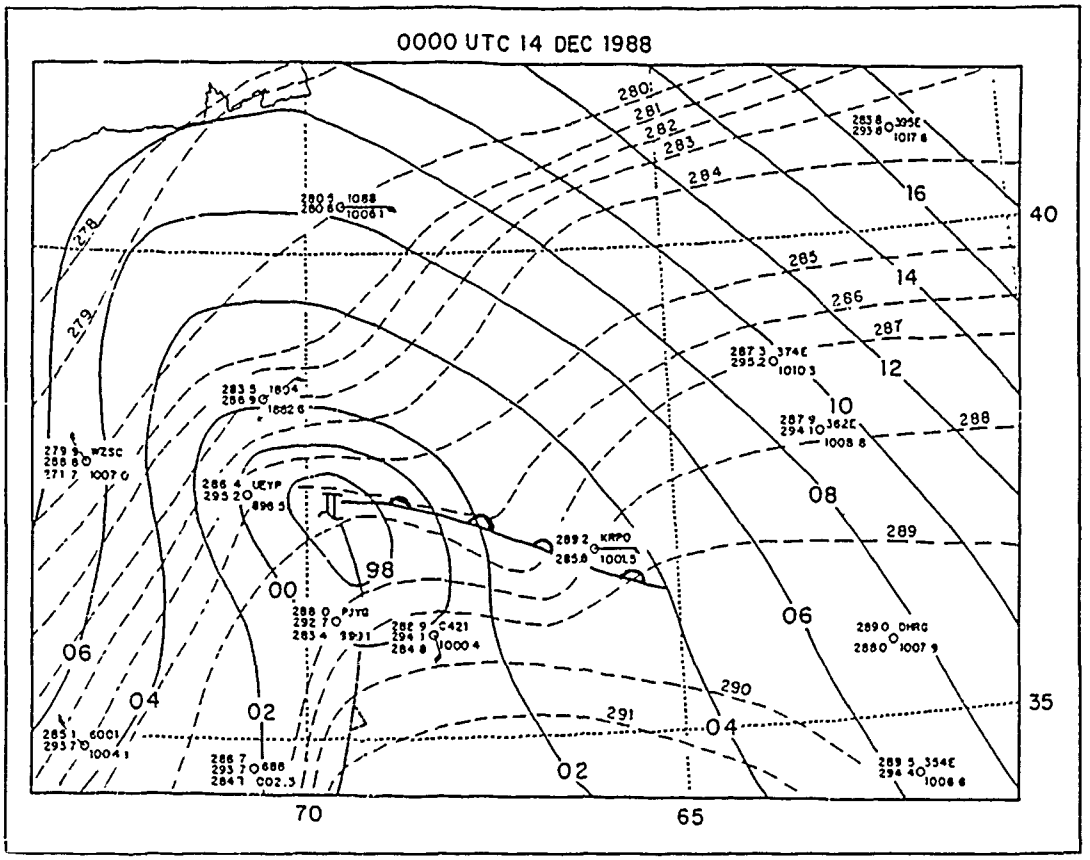

Fig. 11. IOP-2 14/0000 UTC December 1988 mesoscale surface frontal analysis: Sea-level pressure (solid) in mb and surface temperature (dashed) in °C.

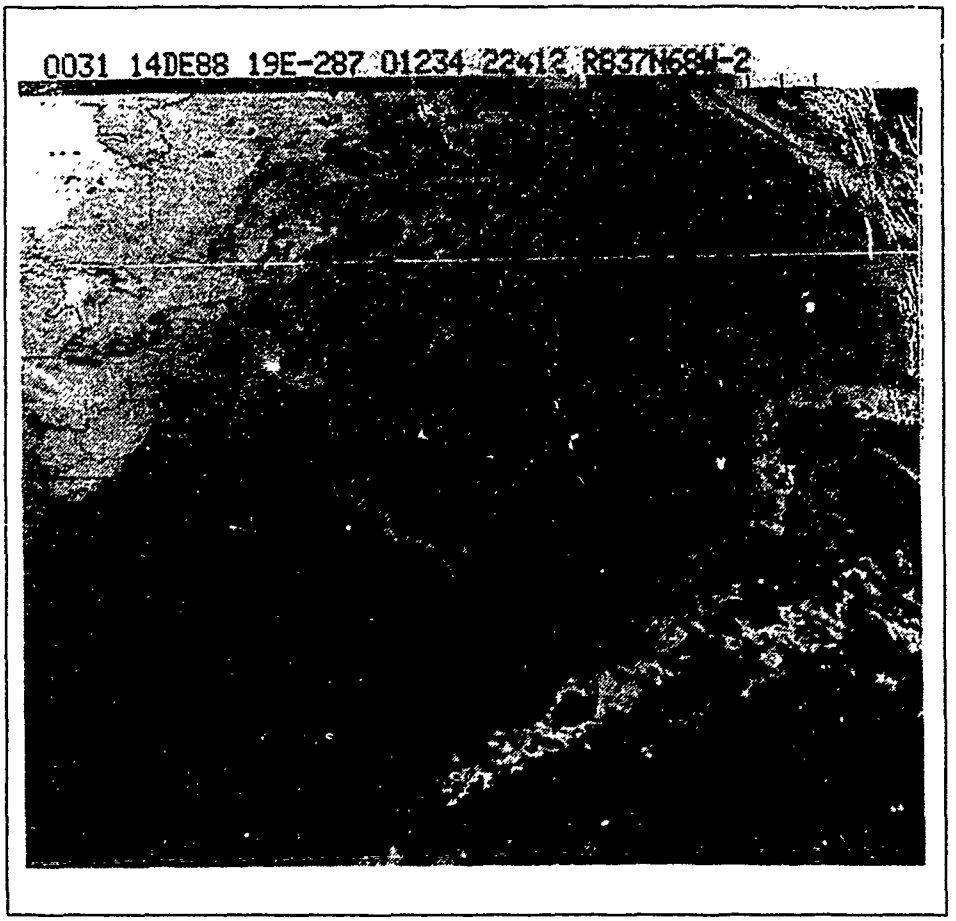

Fig. 12. GOES IR imagery for 14/0031 UTC December 1988: U.S. East Coast sector.

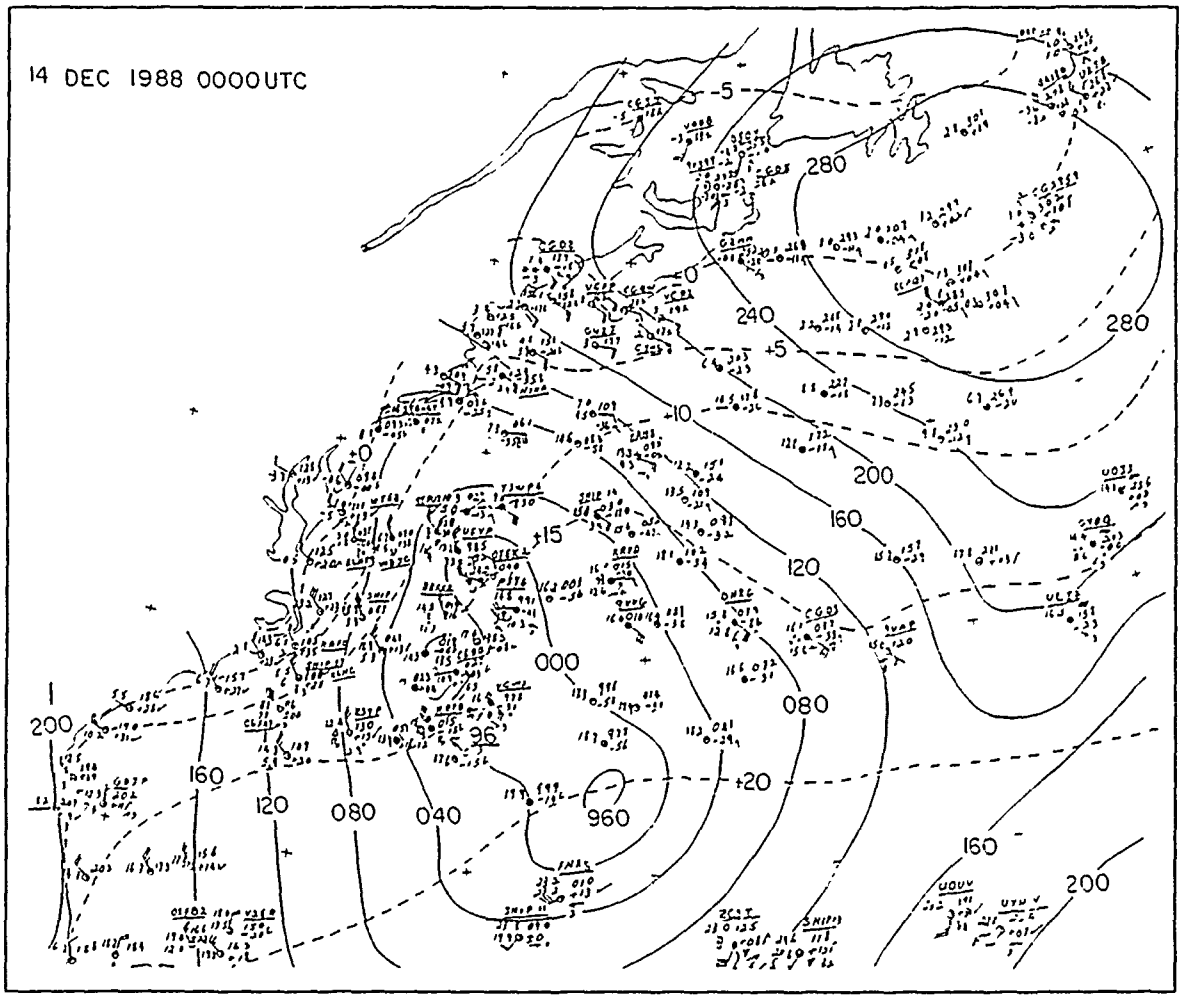

Fig. 13. **IOP-2 14/0000 UTC December 1988 surface analysis:** Sea-level pressure (solid) in tenths of mb where the leading 9 or 10 has been dropped and surface temperature (dashed) in °C (Sanders, 1989).

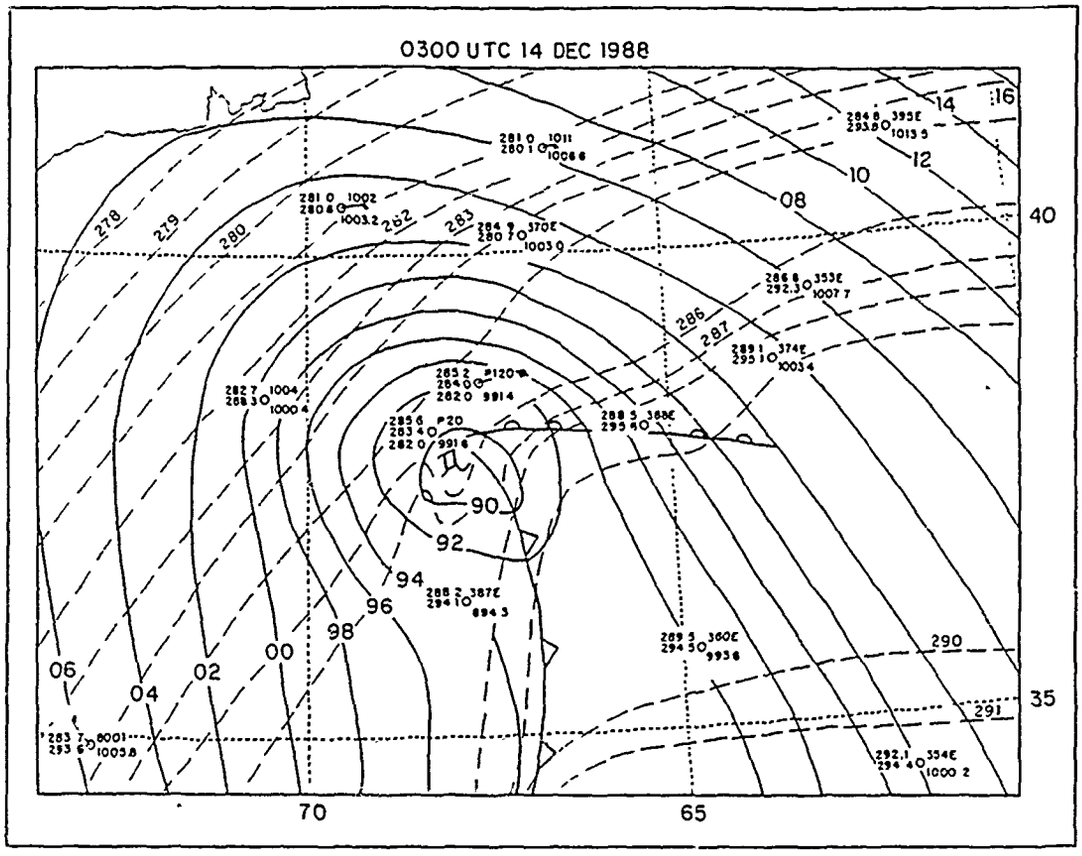

Fig. 14. IOP-2 14/0300 UTC December 1988 mesoscale surface frontal analysis: Sea-level pressure (solid) in mb and surface temperature (dashed) in °C.

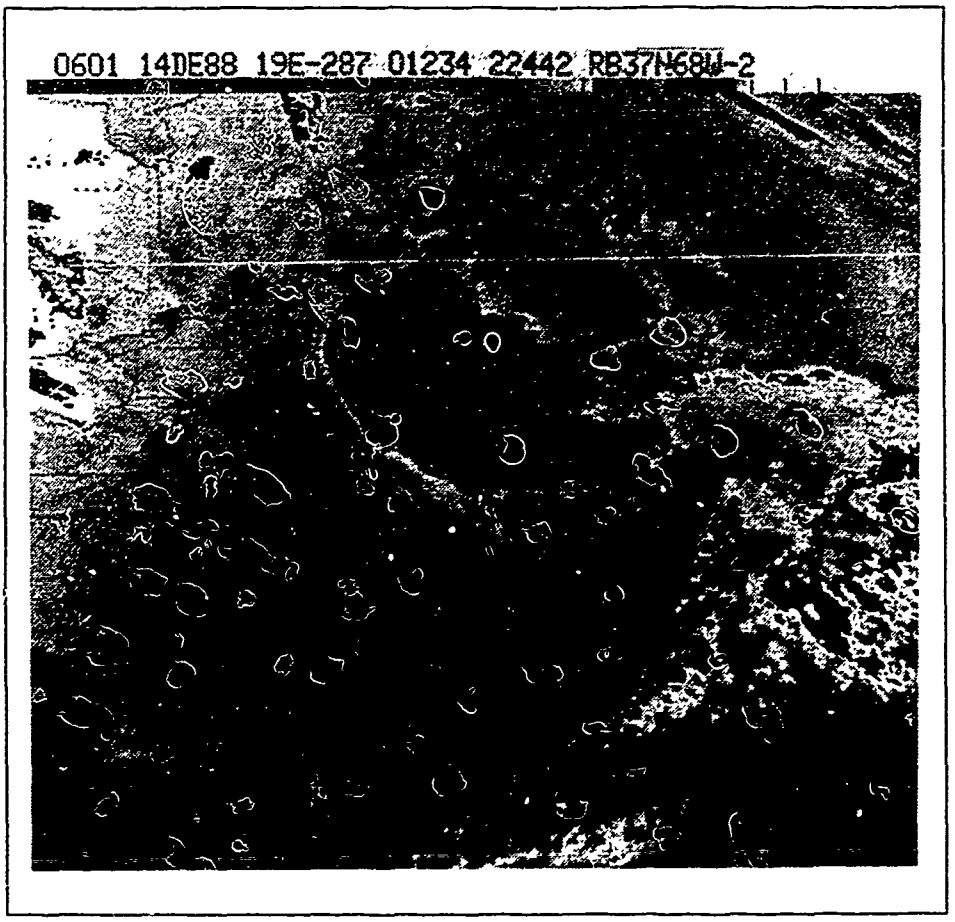

Fig. 15. GOES IR imagery for 14/0601 UTC December 1988: U.S. East Coast sector.

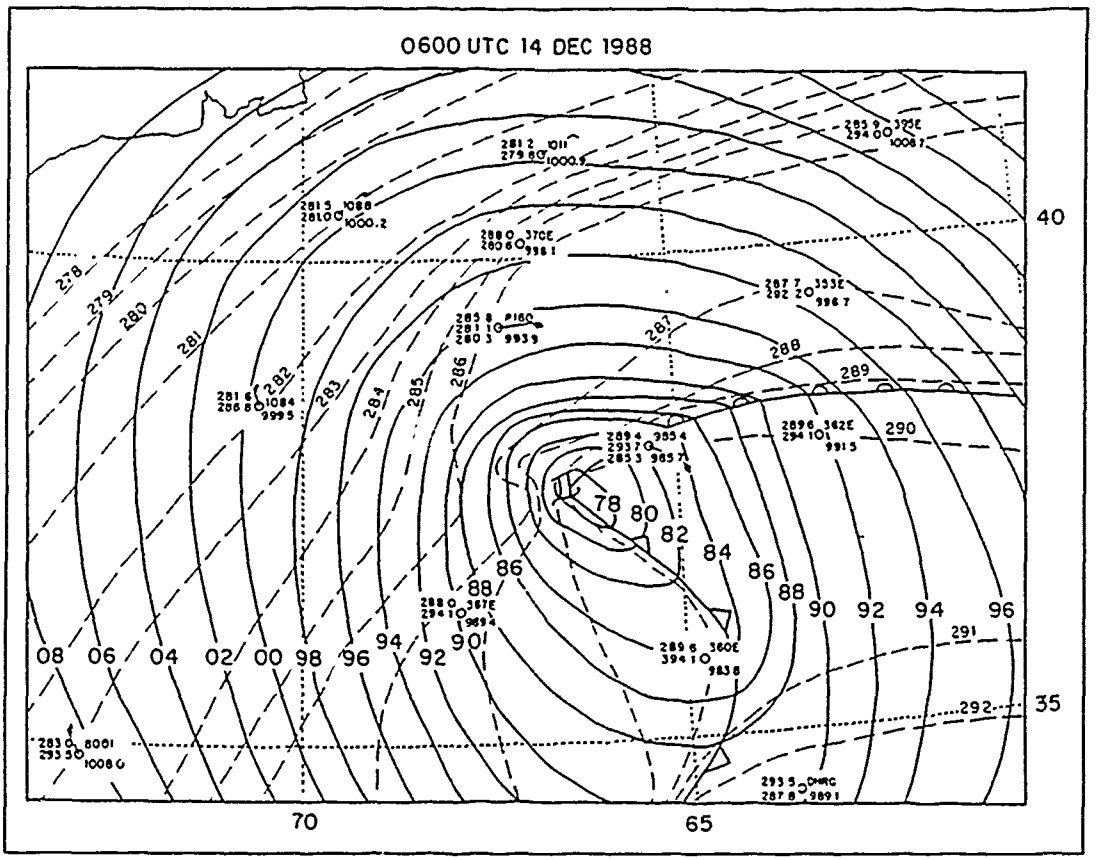

Fig. 16. IOP-2 14/0600 UTC December 1988 mesoscale surface frontal analysis: Sea-level pressure (solid) in mb and surface temperature (dashed) in °C.

Fig. 17. GOES IR imagery for 14/1231 UTC December 1988: U.S. East Coast sector.

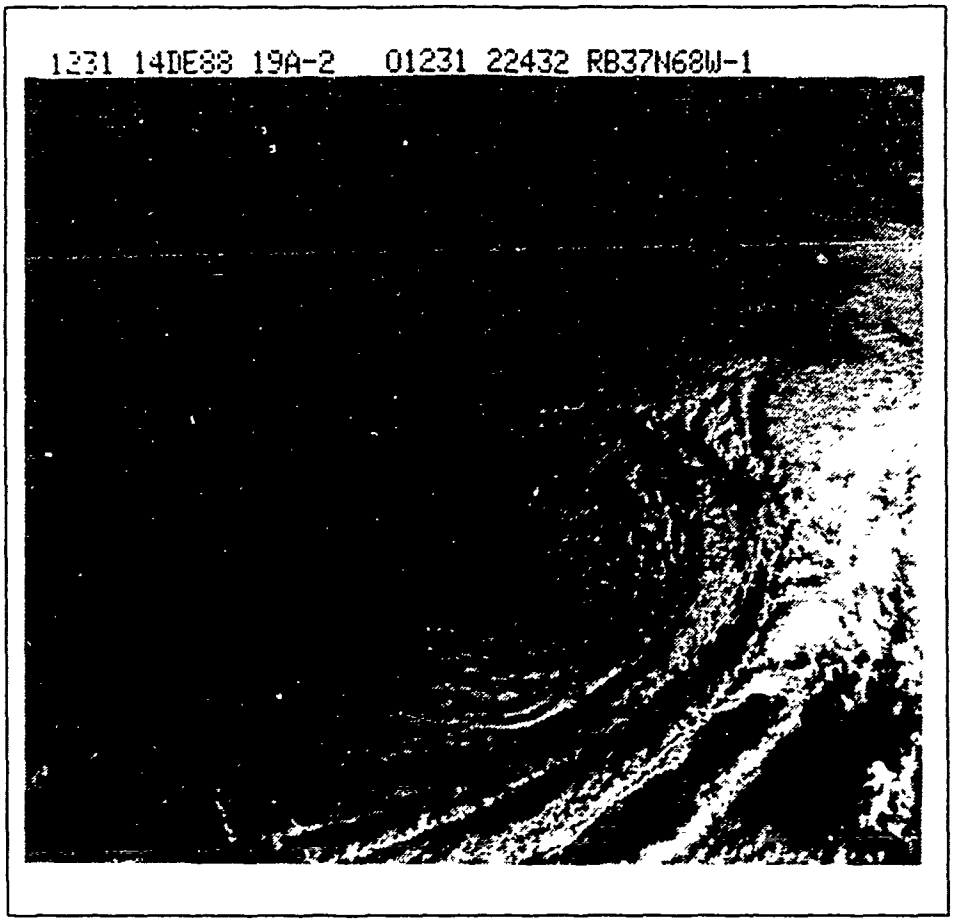

Fig. 18. GOES VIS imagery for 14/1231 UTC December 1988: U.S. East Coast sector.

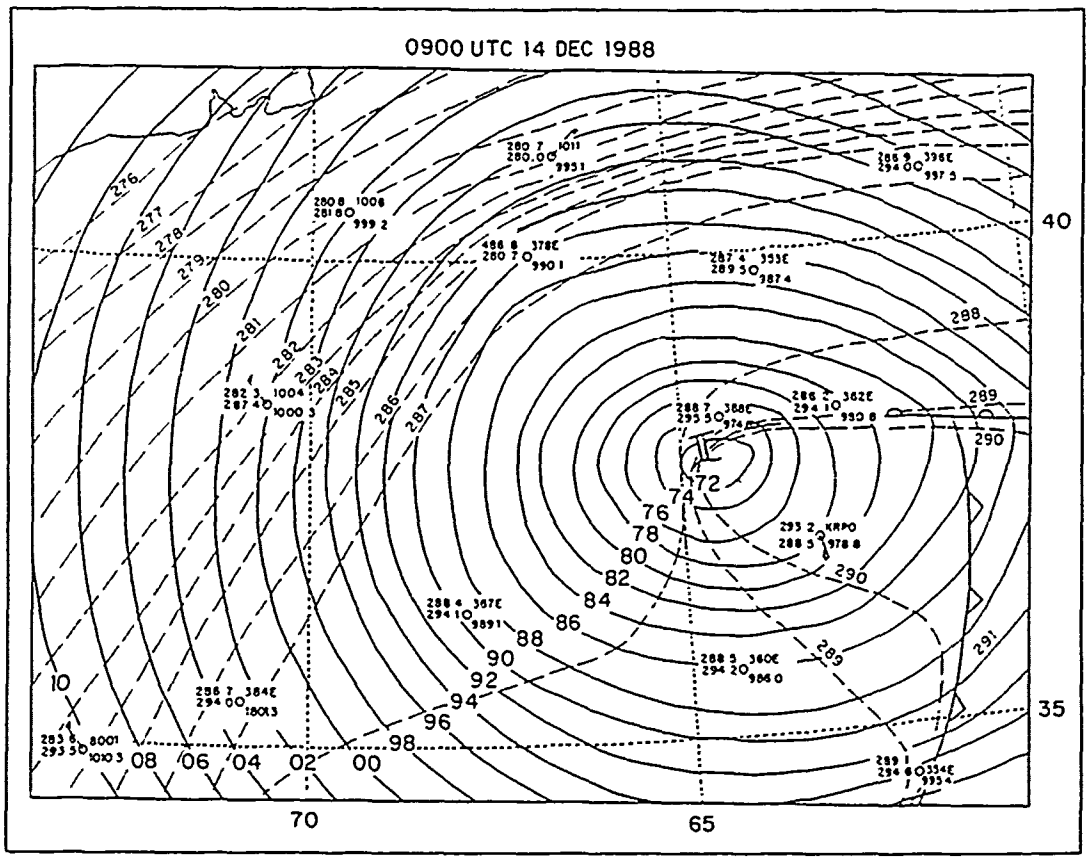

Fig. 19. IOP-2 14/0900 UTC December 1988 mesoscale surface frontal analysis: Sea-level pressure (solid) in mb and surface temperature (dashed) in °C.

V. ANALYSIS OF IOP-2 SURFACE FLUXES

A primary goal of this thesis is to derive the heat flux fields associated with the mesoscale surface structure and to interpret their potential contribution to the cyclogenesis in the IOP-2 cyclone. As discussed in Chapter III, the surface fluxes were calculated from gridded versions of the mesoscale analyses using the Brown-Liu (1982) boundary layer model. These model-generated fluxes provide one estimate of the actual surface fluxes, and provide insight into the basic character of the air-sea interaction in the IOP-2 cyclone.

The mesoscale analysis of IOP-2 described in the previous chapter reveal two important aspects of the low-level structure that influence the air-sea interaction and its evolution. First, the presence of strong, low-level easterly flow to the east of the cyclone tended to reduce the magnitude of the warm advection at the surface during the early stages of development. Second, this low-level easterly flow was colder than the underlying ocean. This air-sea temperature difference evidently caused the air to be strongly modified by surface heat and moisture fluxes.

The lack of warm advection to the east of the low during the early hours of the storm's lifecycle is supported qualitatively by the isotherm pattern and wind observations discussed in the last chapter. To quantify this observation, the thermal advection ($-\vec{v} \cdot \nabla T$) pattern was calculated by using the surface winds produced by the Brown-Liu PBL model and the gridded isotherm analyses. Two representative time periods demonstrate the evolution of the surface warm advection. The first period, 13/1500 UTC (Fig. 20), shows that while there is significant cold thermal advection (about 20 K day^{-1}) west of the developing low, warm advection to the east occurs only in a limited area near the center of the cyclone. At 14/0300 UTC (Fig. 21), 12 h later, the winds around the low have increased with the tightening of the pressure gradient, and the region west of the low shows a four-fold increase in cold advection (to about 80 K day^{-1}). The region to the east shows weak to moderate warm advection (0-20 K day^{-1} over most of the region), which is a much smaller increase than in the cold advection region. The strongest warm advection occurs well to the north of the warm front along the baroclinic zone associated with the Continental Shelf Break Front. These analyses indicate that the region east of the IOP-2 low is characterized by relatively weak surface warm advection during the period prior to rapid deepening as compared to the cold

advection west of the low. Once the rapid deepening started, the primary surface warm advection was associated with the easterly flow to the north of the warm front.

The fact that the easterly flow to the east of the cyclone is colder than the ocean surface is supported by two observations. First, both the actual wind observations and the winds generated by the PBL model show that the flow was predominantly easterly, probably originating in the high to the northeast. Fig. 22 depicts the surface wind pattern, as calculated by the PBL model at 13/2100 UTC, which shows that the winds east of the low are southeasterly becoming easterly north of 37°N. Although a trajectory analysis is required to confirm the source of the cold air in this easterly flow, this wind pattern persists throughout the 12 h period prior to rapid deepening, which provides qualitative evidence of that the 2-D trajectories originate to the northeast of the low. Second, Table 3 shows that the low-level air temperature in the warm sector of the cyclone (taken at the location of meteorological Buoy 360E at 36°N, 65°W) changed very slowly, warming only 6°C in the 12 h prior to explosive development. Although warm temperature advection potentially accounts for this local change in the surface temperature, the large air-sea temperature differences at the buoy indicate that substantial surface warming by the heat fluxes is also occurring. This point will be discussed in greater detail later in this chapter. Both of these observations support an inflow of air much colder than the ocean, which set up the potential for strong positive heat fluxes to the east of the cyclone.

To further support this point, the time-rate of change of temperature ($\partial T/\partial t$) was calculated over each 3-h period. A representative plot of the 3 h change in temperature T for the period 13/1500 - 13/1800 UTC is shown in Fig. 23. The figure shows that the rate of increase in T to the east of the low during this period of early development was substantial (1.8-2.4 $K(3\ h)^{-1}$), with the largest increases in the region just north of the warm front. By comparison, the change in T is substantially less near the center of the cyclone. This provides evidence that the dramatic increase in T in the surface layer to the east of the low observed at the buoy is occurring over a wide region. This is associated with the inflowing cold air to the east, which is warmed and moistened through contact with the relatively warm sea surface.

To better establish the role of heat fluxes in changing the temperature of the surface layer east of the low, the distribution and evolution of surface heat and moisture fluxes were examined. The Brown-Liu PBL model was used to calculate these fluxes, and the results are shown in Fig. 25 through Fig. 30, as well as Table 3. The latent and sensible fluxes appear to be quite consistent throughout the 24-h period of observation, even

Table 3. WARM SECTOR AIR-SEA TEMPERATURE DIFFERENCES AND HEAT FLUXES (36°N,65°W)

Date/Time (UTC December 1988)	Air Temp (°C)	Sea Temp (°C)	ΔT (°C)	Q_H ($W\,m^{-2}$) Sensible Heat Flux	Q_E ($W\,m^{-2}$) Latent Heat
13/0600	281.8	294.1	12.3	-	-
13/0900	282.8	294.1	11.3	-	-
13/1200	283.5	294.1	10.6	250	900
13/1500	285.8	294.3	8.5	280	800
13/1800	287.2	294.3	7.1	160	640
13/2100	288.3	294.3	6.0	230	750
14/0000	289.5	294.1	4.6	400	640
14/0300	289.5	294.5	5.0	160	640
14/0600	289.6	294.1	4.5	160	640
14/0900	288.5	294.3	5.8	230	750
14/1200	289.0	294.3	5.3	280	1200

though the air-sea temperature is decreasing. This may be the result of increasing winds during the period of cyclone development. Table 3 shows that at Buoy 360E, the average sensible heat fluxes were 240 $W\,m^{-2}$ and the latent heat fluxes were 770 $W\,m^{-2}$. Surface fluxes west and southwest of the cyclone appear to be consistently positive during the cyclone, reaching values of 600 $W\,m^{-2}$ sensible and 1200 $W\,m^{-2}$ latent. Total fluxes east of the cyclone are about 1012 $W\,m^{-2}$ at any given time.

A comparison to previous studies of heat fluxes in the vicinity of maritime cyclones provides some perspective on these figures. Petterssen et al. (1962) found that sensible heat fluxes to the west and south of a low may reach a maximum of 700 $W\,m^{-2}$ (about the same for latent heat). He also found that heat fluxes east of the low are 1-2 orders of magnitude less, though generally not becoming negative.

More recently, Nuss and Kamikawa (1990) found that the surface heat fluxes of a non-explosive eastern North Pacific cyclone were -30 $W\,m^{-2}$ east of the low (both sensible and latent). Heat fluxes west of the low, however, were +330 $W\,m^{-2}$ and +900 $W\,m^{-2}$ for sensible and latent fluxes, respectively. These results were in contrast to an explosively deepening cyclone in the same waters which occurred a few days later,

showing + 100 $W\,m^{-2}$ sensible and + 80 $W\,m^{-2}$ latent heat fluxes east of the low (with little significant change to the west).

The actual distribution of heat fluxes in the vicinity the IOP-2 storm show a similar tendency to remain large over the entire region throughout the development. Steeley (1990) demonstrated in a single "snapshot" analysis of IOP-2 at 14/0600 UTC that there were strong positive heat fluxes east of the low. The heat fluxes for 13/1200 UTC (Fig. 25 and Fig. 26) show that a region of strong positive (480 $W\,m^{-2}$ sensible and 1160 $W\,m^{-2}$ latent) heat fluxes exist in the region along and to the south of the Gulf Stream, comparable to those found by Steeley (1990) at a later time. (Note that this discussion of the evolution of the IOP-2 heat fluxes is in the Lagrangian frame, with reference to the warm sector of the cyclone and the warm front.) Comparison with later time periods show that while the heat fluxes in the vicinity of the warm front remain strongly positive throughout the storm's lifecycle, this early period (the 12 h prior to rapid deepening) features the strongest fluxes. This result is completely consistent with Kuo et al. (1990), who showed through numerical simulations that surface energy fluxes are important throughout the lifecycle of a "bomb", and not just during the rapid deepening phase. This is also consistent with the air-sea temperature difference tendency observed at the buoy (Table 3). It is evident from GOES IR and visible imagery (Fig. 4 and Fig. 5) that a large region of convective activity exists over the region to the south and east of the incipient cyclone. This strongly suggests a substantial degree of potential instability in the boundary layer early in the development of IOP-2.

By 13/1800 UTC (Fig. 27 and Fig. 28) the frontal zones have become well-established, and a region of maximum positive fluxes is found in the warm sector of the cyclone, behind the warm front. Flux intensities have diminished slightly by this time, especially the sensible heat flux, which is now half of its value of 6 h earlier. The latent heat fluxes are undiminished compared to the earlier time. There are several areas of strong positive fluxes north of the Gulf Stream, which are located directly over a pair of warm core eddies (WCE's).

During the period of most rapid deepening the fluxes for 14/0600 UTC (Fig. 29 and Fig. 30) show that there are still strong positive fluxes in the warm sector. The darkened "bullseye" regions are points where the PBL model failed to converge to a solution for the surface winds. This was most likely due to the very large geostrophic wind speeds and air-sea temperature differences in some regions of the storm. This is particularly prevalent in the cold air west of the cold front. However, sufficient regions produced

reliable solutions to be able to state that strong positive fluxes in the warm sector south of the warm front occurred throughout the period prior to and during rapid cyclogenesis.

To better quantify the potential role of the fluxes in cyclogenesis, an appropriate question is the degree to which the fluxes alone could reasonably account for the observed temperature changes in the boundary layer. To answer this, a representative calculation is made of the change in temperature for a 1 km deep boundary layer under the influence of a sensible heat flux of 240 $W\,m^{-2}$ (latent heat fluxes should not play a significant role in altering the temperature within the boundary layer). Assuming no horizontal or vertical advection and approximately the vertical flux divergence in the boundary layer as the surface flux is divided by the depth, a local temperature change can be calculated from

$$\Delta T = -\frac{\Delta t}{C_p \rho_a} \frac{\Delta \tilde{Q}_H}{\Delta z}. \tag{14}$$

The typical values stated above yield a temperature change ΔT of 2.1°C, where Δt = 1.08 x 10^3 s (3 h), the specific heat of air $C_{pa} = 1004.67\ J\,kg^{-1}\,K^{-1}$, atmospheric density $\rho_a = 1.225\ kg\,m^{-3}$, $\Delta z = 10^3\ m$, and the change in sensible heat flux with height $\Delta \tilde{Q}_H = 240\ W\,m^{-2}$. Another way of looking at this result is to say that a 100 $W\,m^{-2}$ positive heat flux results in a 0.9°C temperature rise in the boundary layer. This demonstrates that heat fluxes alone could account for a 2°C temperature rise in a 1 km deep boundary layer in 3 h, which is very consistent with the $1.3°C\,(3\ h)^{-1}$ rate of surface temperature increase observed in IOP-2 prior to 14/0000 UTC (Table 3).

Doppler radar aboard ERICA research aircraft observed convective activity along the warm front as high as 5 km, which indicates that the heating may be mixed through a much deeper layer. However, latent heat release certainly becomes a factor in the thermal modification under these circumstances, which is not accounted for in this simple estimate. In fact, a layer as deep as 2-3 km would bring the calculated ΔT value even closer to the increase actually observed. It is certainly possible to account for a large fraction of the observed warming of the boundary layer by surface heat fluxes alone in this case.

The warming trend in the warm sector boundary layer was, in fact, remarkably consistent during the period prior to rapid deepening. Fig. 24 graphically depicts the change in air-sea temperature differences (ΔT) over time, which is actually a measure of the warming of the boundary layer, since the SST is effectively unchanged during the

period of the study. The graph shows that there is a slow but steady increase in atmospheric temperature (reduction in ΔT) during the first 18 h of the storm's development, and that the rate of warming fell off after rapid development began, around 14/0000 UTC. Fig. 24 indicates that the hourly rate of temperature change is constant at -0.43 $K\,h^{-1}$ in the period 13/0600 - 14/0000 UTC, dropping down to almost no change (-0.04 $K\,h^{-1}$) in the 18 h following the onset of explosive deepening. It should be noted that the cold front does not pass over Buoy 360E until 14/0600 UTC, 6 h after the break in the earlier trend line; however the buoy is in a region that is subject to substantial wind stress as the low deepens, which would certainly have a profound effect on boundary layer processes during that time. The consistency with which the heating of the boundary layer occurs and the nearly constant large heat flux argues in favor of a significant role for heat fluxes in the warm sector of the IOP-2 cyclone.

Ultimately, the heat flux and baroclinic conditions described above led to convergent flow along the warm front, resulting in vertical motion that lifts the flux-modified air from the surface into the cloud regions, which may contribute to rapid cyclogenesis. The convergent flow at the surface along the warm front can result from a variety of contributing factors, particularly the frictional and thermal wind turning in the boundary layer, among others. Fleagle and Nuss (1985) noted that if the acceleration terms of the vorticity equation are small, then the vertical motion at the top of the boundary layer depends primarily on frictionally-driven convergence, that is given by the curl of the surface stress, which is dependent upon horizontal variations in wind stress. The following discussion is somewhat speculative, but it is based on the characteristics of IOP-2 that have been elucidated in this thesis, and observations by others of other rapidly deepening cyclones.

The warm frontal structure of a typical cyclone characterized by strong low-level warm advection would result in a comparatively stable boundary layer behind the front, in the warm sector, and a well-mixed layer capped by a frontal inversion ahead of the front. However, IOP-2 featured very strong positive heat fluxes to the south of the warm front that led to substantial warming and moistening (and presumably destabilization) of the updraft region of the warm front. The resultant vertical motion along the warm front is believed to have caused the zone behind the warm front to become well-mixed to a significant depth, much more so than would have been found in a cyclone that experienced net downward fluxes in the same region. To the north of the Gulf Stream, comparatively weaker surface heating may have resulted in a somewhat more stable PBL in that region. This result contradicts the findings of Nuss (1989), whose

numerical model study predicted a stably stratified boundary layer in the warm sector. This structure is also very different than that found by Nieman et al. (1990) for a cyclone that moved across the Gulf Stream. The differential momentum transfer to the north and south of the Gulf Stream possibly contributed to frictional convergence at the front in the IOP-2 cyclone; however, this remains to be established in a future study.

It should be emphasized that the air-sea interaction in the IOP-2 cyclone apparently differs substantially from a typical cyclone. In a typical cyclone, the region east of the cyclone is usually characterized by strong surface warm advection and downward heat fluxes, leading to a reduction in baroclinity (Petterssen et al., 1962 and Fleagle and Nuss, 1985). However, in the IOP-2 cyclone, the SST pattern associated with the Gulf Stream and the overlying air temperature patterns were "in phase" with each other, a pattern which Nuss (1989) has demonstrated in numerical simulations to result in strong positive upward heat fluxes northeast as well as west of the developing low. Nuss (1989) found that cyclones with "in phase" thermal patterns deepen more rapidly in numerical simulations than typical cyclones where warm air advection results in negative fluxes east of the low. In order for this "in phase" temperature pattern to exist and be maintained in the IOP-2 cyclone, the cold air outbreak behind an earlier cyclone and the low-level easterly flow were important.

The fact that the warm front remained aligned along the Gulf Stream throughout the cyclogenesis supports the interpretation of little surface warm advection from the south. In the absence of strong northward warm advection, the confluent easterly flow along the Gulf Stream was not substantially altered throughout the development. This confluent flow was continually being warmed and moistened by the surface fluxes. This air was subsequently lifted above the PBL to a level where the latent heat could be released, presumably deepening and propagating the cyclone at an accelerated rate. This pattern of persistent surface interaction in the IOP-2 cyclone is significant as it suggests contributions by the surface fluxes throughout the development. This differs from the results of Kuo et al. (1990) which indicate that the surface energy fluxes had a much stronger effect in the early period of storm development than during the rapid cyclogenesis stage. The full significance of the role of surface heat fluxes and frontal dynamics in rapid cyclogenesis needs to be determined and a number of lines of future research have suggested themselves in its preparation. These recommendations will be addressed in Chapter VII.

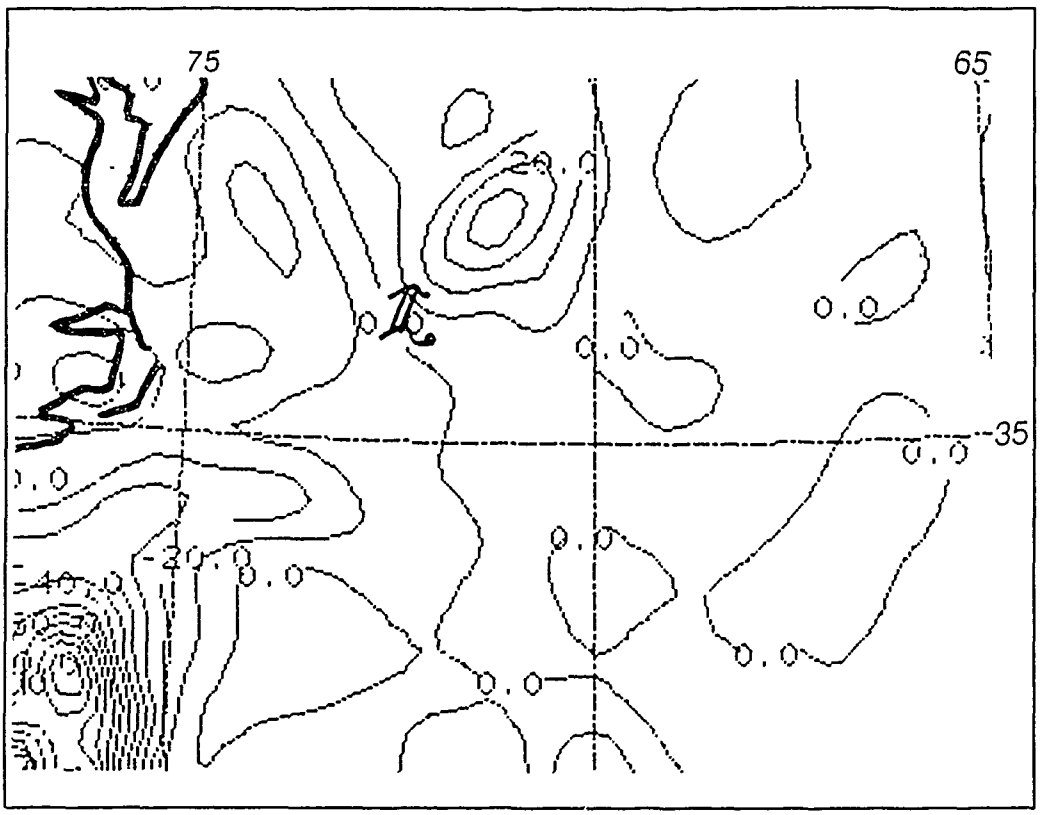

Fig. 20. Thermal advection at 13/1500 UTC December 1988: in intervals of 10 $K\ day^{-1}$.

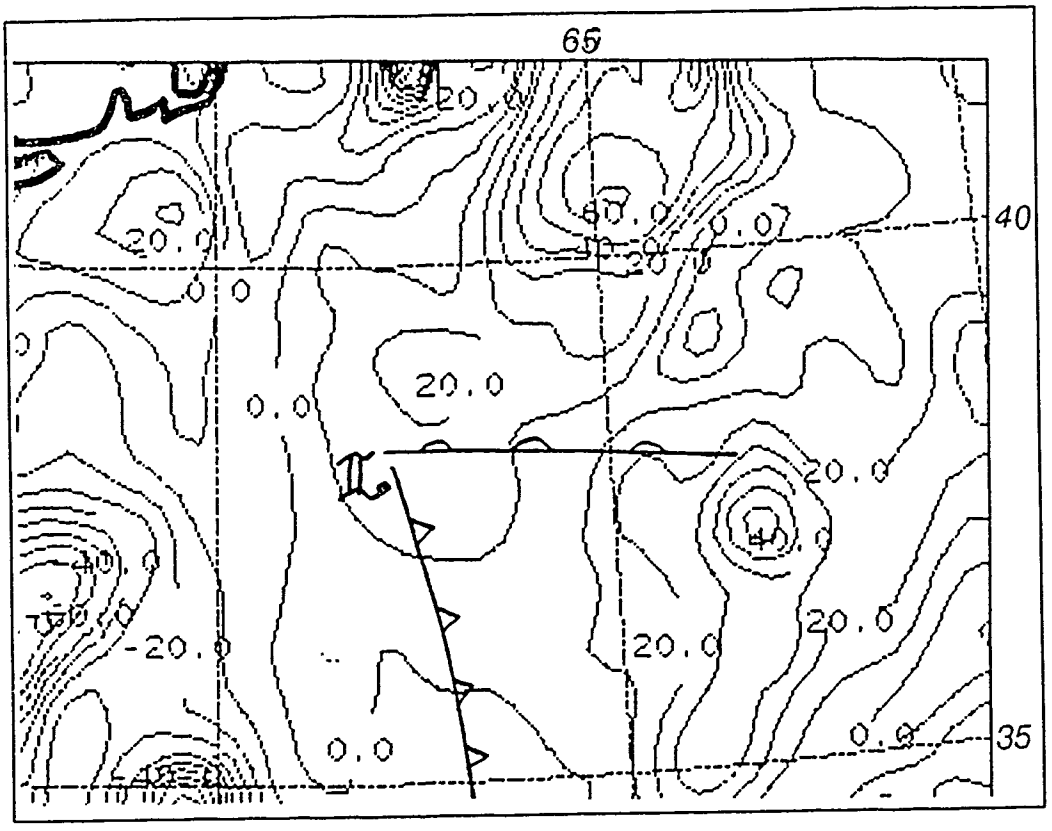

Fig. 21. Thermal advection at 14/0300 UTC December 1988: in intervals of 10 $K\ day^{-1}$.

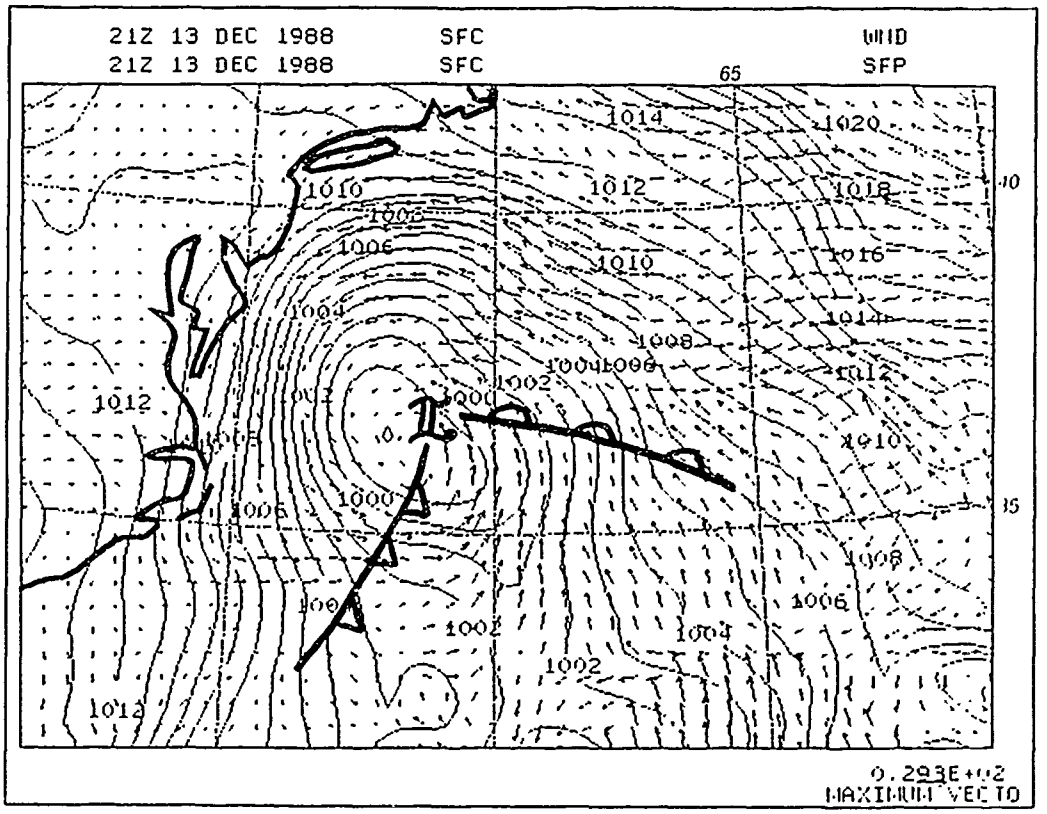

Fig. 22. Surface level winds and isobars for 13/2100 UTC December: pressure in intervals of 2 mb.

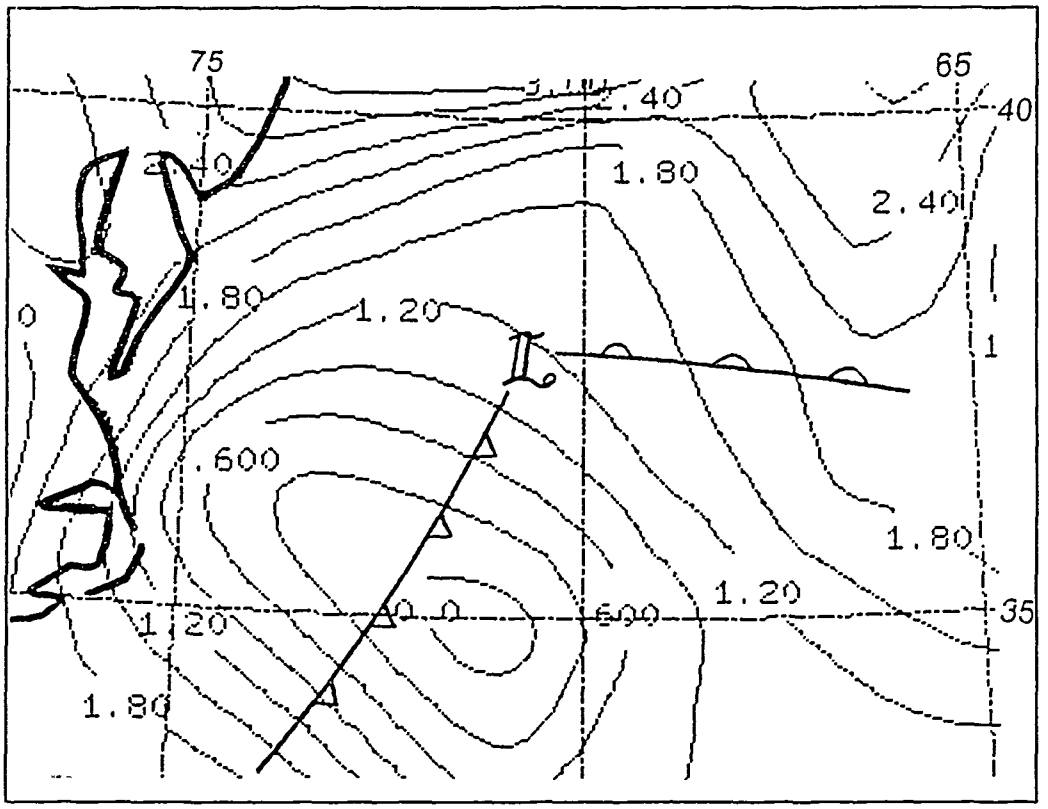

Fig. 23. 3 h change in surface temperature (13/1500 -13/1800 UTC): in intervals of $K\,day^{-1}$.

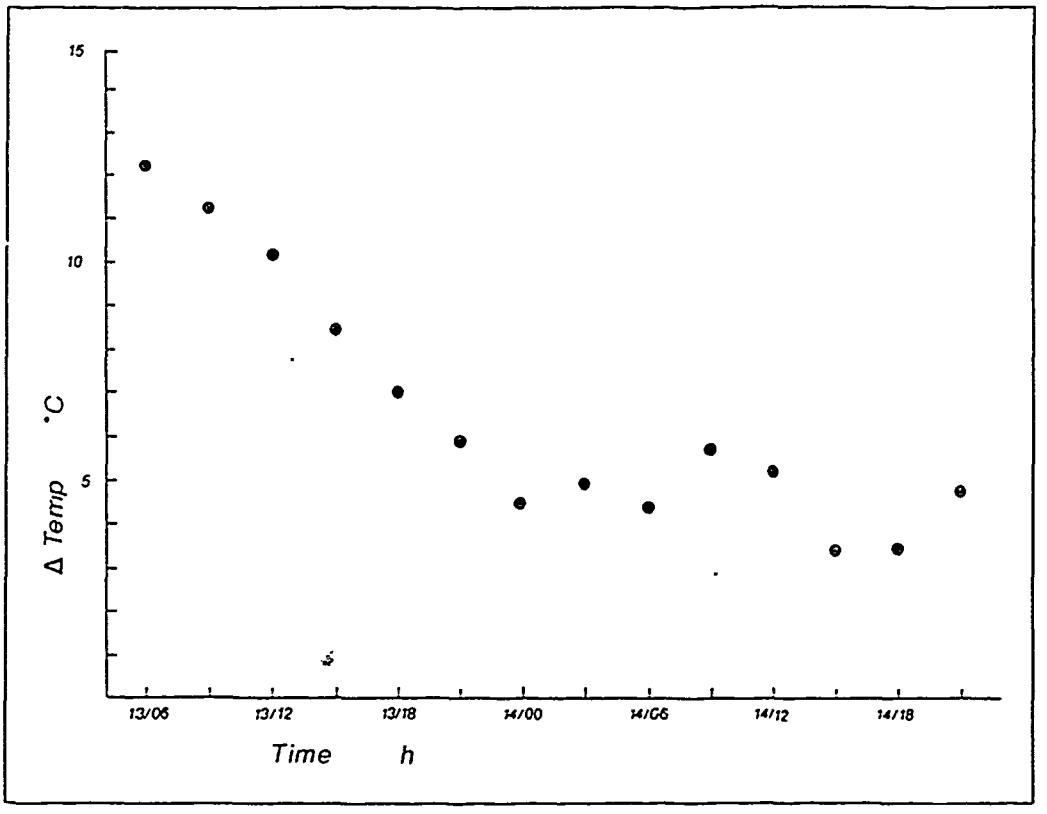

Fig. 24. Time-rate of change of air-sea temperature differences: taken at Buoy 360E (36°N, 65°W) in the warm sector of IOP-2.

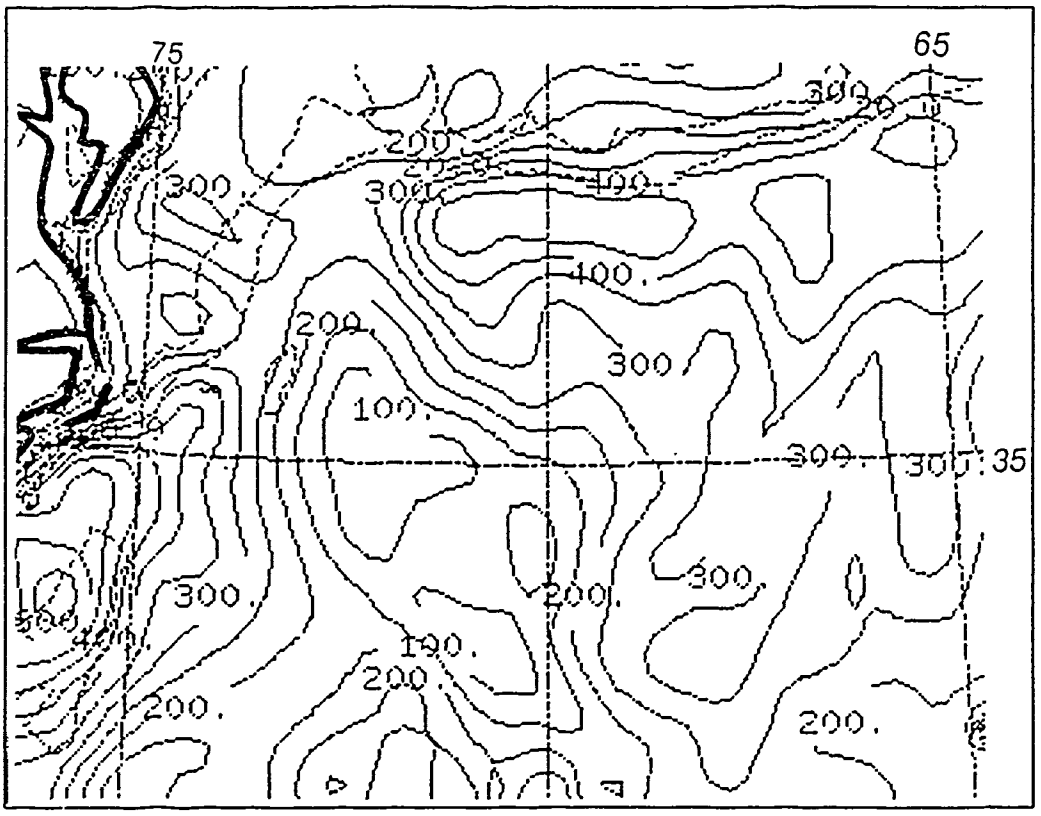

Fig. 25. Sensible heat fluxes for 13/1200 UTC: Sensible heat fluxes in intervals of 100 $W\,m^{-2}$, SST (dashed) in °C.

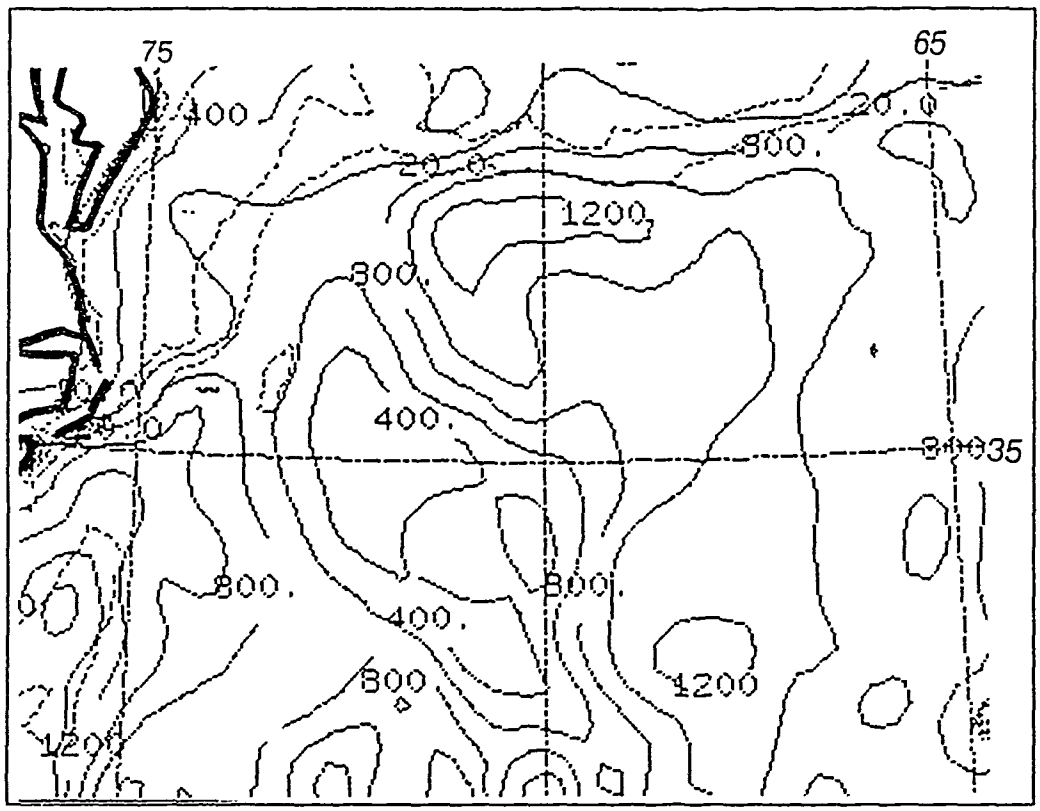

Fig. 26. **Latent heat fluxes for 13/1200 UTC:** Latent heat fluxes in intervals of 200 $W\ m^{-2}$, SST (dashed line) in °C.

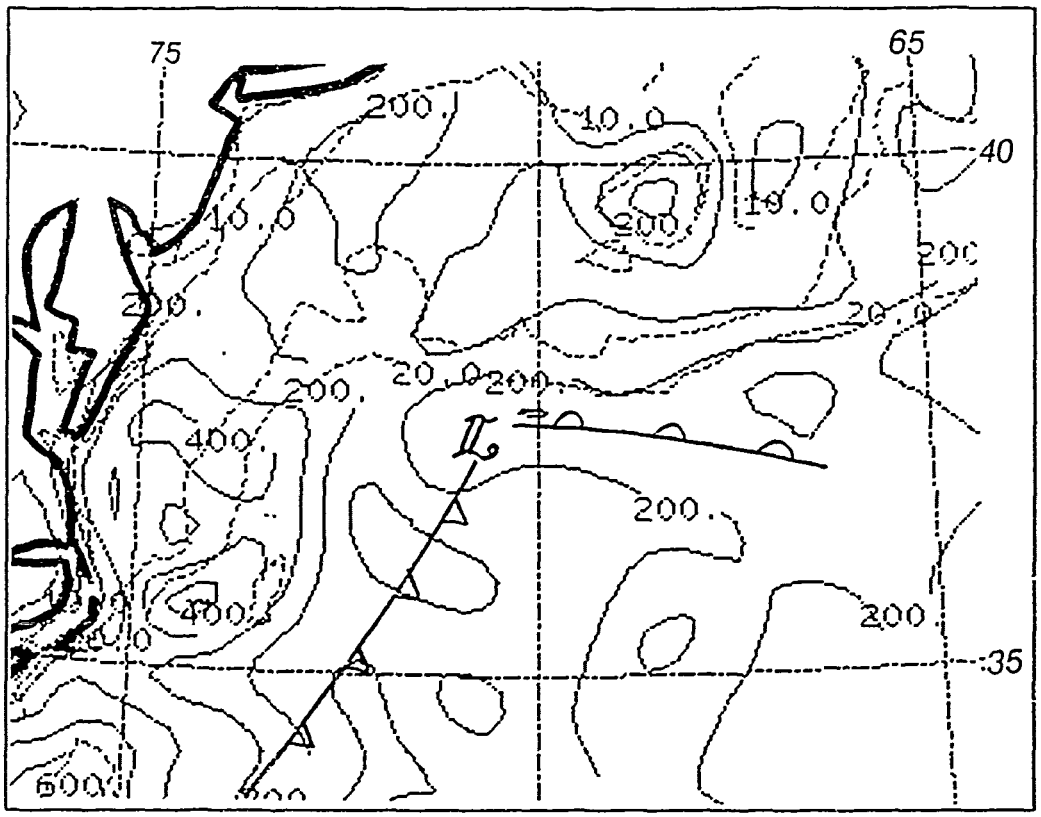

Fig. 27. Sensible heat fluxes for 13/1800 UTC: Sensible heat fluxes in intervals of 100 $W m^{-2}$, SST (dashed) in °C.

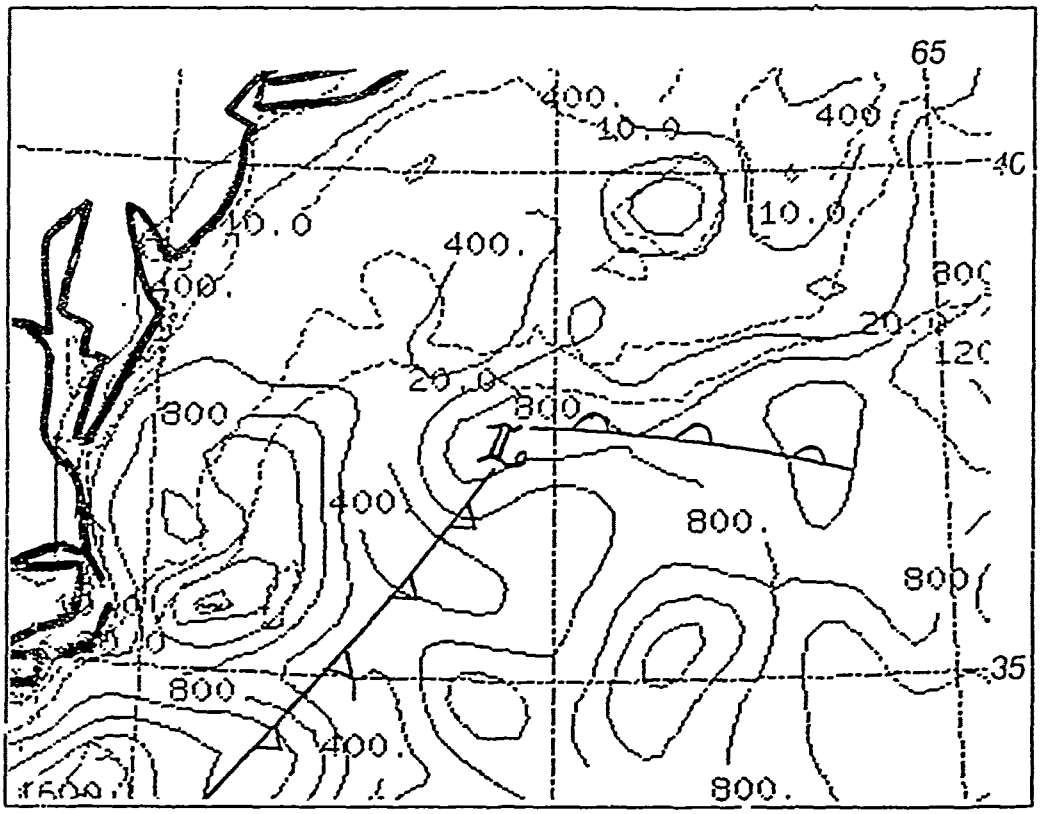

Fig. 28. Latent heat fluxes for 13/1800 UTC: Latent heat fluxes in intervals of 200 $W\,m^{-2}$, SST (dashed) in °C.

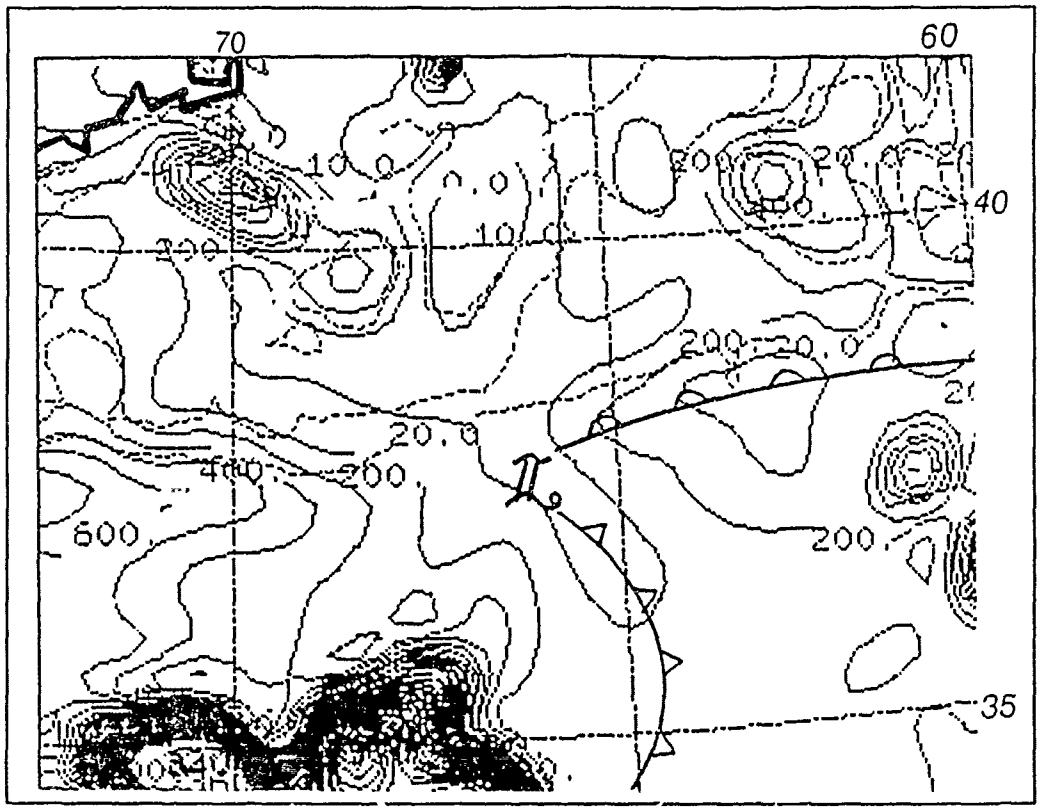

Fig. 29. Sensible heat fluxes for 14/0600 UTC: Sensible heat fluxes in intervals of 100 $W\,m^{-2}$, SST (dashed) in °C.

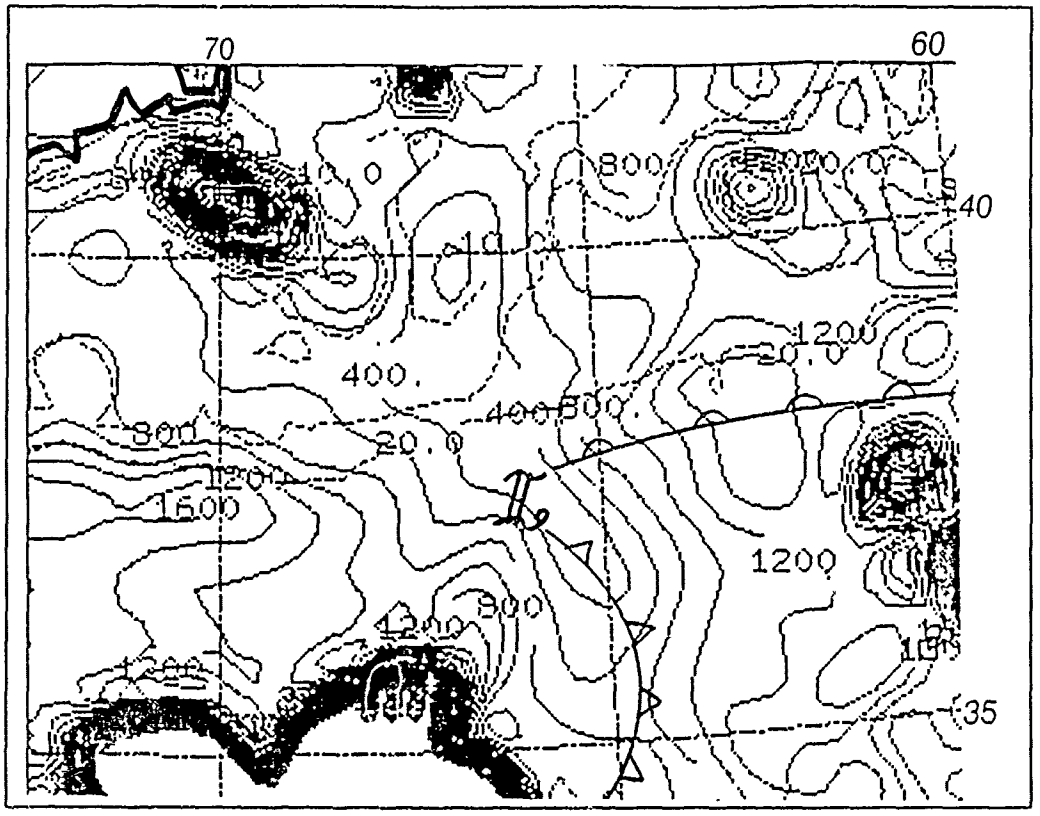

Fig. 30. **Latent heat fluxes for 14/0600 UTC:** Latent heat fluxes in intervals of 200 $W\,m^{-2}$, SST (dashed) in °C.

VI. CONCLUSIONS

The IOP-2 cyclone was a rapid deepener which developed a central pressure of 968 mb after only 24 h, a deepening rate of 2.34 B. A mesoscale analysis of the low and frontal structure, and calculations of the surface latent and sensible heat fluxes lead to the following conclusions:

1. Heat flux calculations, using the bulk method, showed that there was substantial warming of the air in the warm sector of the storm due to heat fluxes. The relative contribution to surface warming by warm air advection and the heat flux could not be accurately determined but may have been comparable to or dominated by the surface heat flux.
2. A low-level easterly flow was characterized by a large air-sea temperature difference which allowed the large positive heat fluxes to persist throughout the period of the storm's development.
3. The storm developed along the north boundary of the Gulf Stream, providing the conditions for air temperature and SST patterns to be in phase, which has been shown in model studies to be conducive to accelerated development rates.
4. The entire 24 hours of the storm's development, especially the 12 h prior to explosive deepening, were marked by strong upward latent and sensible heat fluxes east and northeast of the cyclone. This strongly suggests that heat fluxes in the period before rapid development play a critical role in preconditioning the region in advance of the storm, and reducing the static stability of the low-level air mass in the warm sector.
5. The potentially unstable (high θ_e) air in the warm sector, which resulted from the strong positive heat fluxes in the hours prior to rapid development, was forced aloft by the PVA associated with a 500 mb shortwave trough. This resulted in a large region of convective activity and low-level convergence, especially in the vicinity of the developing warm front.
6. The IOP-2 storm and its warm front remained in the vicinity of the Gulf Stream throughout the period of rapid deepening. This was the result of a balance between the lack of strong northward surface warm air advection behind the warm front, and strong surface frontogenesis along the Gulf Stream possibly as a result of boundary layer effects on the ageostrophic flow.

VII. RECOMMENDATIONS

This thesis has addressed only a few of the many questions involving explosively deepening cyclones. Listed below are some of the avenues of research that were suggested by this work:

- Perform similar mesoscale analyses of other ERICA cyclones, looking specifically for evidence of a strong baroclinic zone tied to the Gulf Stream, a consistent source of low θ_e air, and weak warm advection.
- Perform mesoscale analyses at other levels of IOP-2, above the boundary layer, so that a true vertical picture of the cyclone and warm frontal structure can be determined and the relative contribution of the surface fluxes moree accurately assessed.
- Generate divergence fields in the boundary layer in order to quantify the location and amount of greatest frontal convergence and frontogenesis.
- Perform static stability calculations for the period of the cyclone.
- Conduct numerical model experiments with the PSU/NCAR model, in an attempt to duplicate the mesoscale conditions described in this study.
- Evaluate available dropwindsonde data to determine potential instability and vorticity across the warm front.
- Examine air parcel trajectories to confirm the source of the air lifted in the warm frontal zone.

LIST OF REFERENCES

Brown, R. A. and W. T. Liu, 1982: An operational large-scale marine planetary boundary layer model. *J. Appl. Meteor., 21,* 261-269.

Carlson, T. N., 1980: Airflow through midlatitude cyclones and the comma cloud pattern. *Mon. Wea. Rev., 108,* 1498-1509.

Chalfant, A., 1989: Dynamics of an ERICA cyclone. Master's thesis, Naval Postgraduate School, Monterey, CA, 55 pp.

Cressman, G. R., 1959: An operational objective analysis system. *Mon. Wea. Rev., 87,* 367-374.

Davis, C. A. and K. A. Emanuel, 1988: Observational evidence for the influence of surface heat fluxes on rapid maritime cyclogenesis. *Mon. Wea. Rev., 116,* 2649-2659.

Emanuel, K. A., 1983: Observational evidence of slantwise convective adjustment. *Mon. Wea. Rev., 116,* 1805-1816.

Fleagle, R. G., and W. A. Nuss, 1985: The distribution of surface fluxes and boundary layer divergence in midlatitude ocean storms. *J. Atmos. Sci., 42,* 784-799.

Hadlock, R., and C. W. Kreitzberg, 1988: The experiment on rapidly intensifying cyclones over the Atlantic (ERICA) field study: objectives and plans. *Bul. Am. Met. Soc., 69,* 1309-1320.

Holton, J. R., 1979: *An Introduction to Dynamic Meteorology.* Academic Press, Inc., New York, 391 pp.

Kocin, P., and L. Uccellini, 1985: A survey of major East Coast snowstorms 1960-1983. Part I: Summary of surface and upper-level characteristics. NASA Tech. Memo. 86196, NASA/Goddard Space Flight Center, Greenbelt, MD

Kuo, Y. H., R. J. Reed, and S. Low-Nam, 1990: Effects of surface energy fluxes during the early development and rapid intensification stages of winter cyclones in the Western Atlantic. *Mon. Wea. Rev.* (submitted).

Neiman, P. J., M. A. Shapiro, E. G. Donall and C. W. Kreitzberg, 1990: Diabatic modification of an extratropical marine cyclone warm sector by cold underlying water. *Mon. Wea. Rev., 118,* 1576-1590.

Nuss, W. A., and R. A. Anthes, 1987: A numerical investigation of low-level processes in rapid cyclogenesis. *Mon. Wea. Rev., 115,* 2728-2743.

_____, 1989: Air-sea interaction influences on the structure and intensification of an idealized marine cyclone. *Mon. Wea. Rev., 117,* 351-369.

_____ and S. I. Kamikawa, 1990: Dynamics and boundary layer processes in two Asian cyclones. *Mon. Wea. Rev., 118,* 755-771.

Petterssen, S., 1956: *Weather Analysis and Forecasting: Vol I: Motion and Motion Systems.* 2nd ed. McGraw-Hill, 428 pp.

_____, D. L. Bradbury and K. Pedersen, 1962: The Norwegian cyclone model in relation to heat and cold sources. *Geofys. Publ., 24,* 243-280.

Reed, R. J., and M. D. Albright, 1986: A case study of explosive cyclogenesis in the eastern Atlantic. *Mon. Wea. Rev., 114,* 2297-2319.

Sanders, F., and J. R. Gyakum, 1980: Synoptic-dynamic climatology of the "bomb". *Mon. Wea. Rev., 108,* 1589-1606.

_____, 1986: Explosive cyclogenesis in the west-central North Atlantic Ocean 1981-84. Part I: Composite structure and mean behavior. *Mon. Wea. Rev., 104,* 1781-1794.

_____, 1987: Skill of NMC operational dynamical models in predicting explosive cyclogenesis. *Wea. and Forecasting, 2,* 322-336.

_____, 1989: ERICA surface analysis. Available from ERICA Data Center, Drexel University, Philadelphia, PA.

Shapiro, M. A., and D. Keyser, 1990: Fronts, jet streams and the tropopause. *Extratropical Cyclones* (The Erik Palmen Memorial Volume), C. W. Newton and E. O. Holopainen, Eds., American Meteorological Society, 167-191.

Steeley, G. D., 1990: Boundary layer structure of an explosive cyclone. Master's thesis, Naval Postgraduate School, Monterey, CA, 30 pp.

Stull, R. B., 1989: *An Introduction to Boundary Layer Meteorology.* Kluwer Academic Publishers, Dordrecht, The Netherlands, 666 pp.

Wash, C. H., J. E. Peak, W. E. Calland and W. A. Cook, 1988: Diagnostic study of explosive cyclogenesis during FGGE. *Mon. Wea. Rev., 116,* 431-451.

INITIAL DISTRIBUTION LIST

		No. Copies
1.	Defense Technical Information Center Cameron Station Alexandria, VA 22304-6145	2
2.	Library, Code 52 Naval Postgraduate School Monterey, CA 93943-5002	2
3.	Chairman (Code MR/Hy) Department of Meteorology Naval Postgraduate School Monterey. CA 93943-5000	1
4.	Professor Wendell A. Nuss (Code MR/Nu) Department of Meteorology Naval Postgraduate School Monterey, CA 93943-5000	2
5.	Professor Carlyle H. Wash (Code MR/Wx) Department of Meteorology Naval Postgraduate School Monterey, CA 93943-5000	1
6.	LCDR Craig D. Lilly, USN OA Division, Operations Department USS DWIGHT D. EISENHOWER (CVN-69) FPO New York, NY 09532-2830	1
7.	Commander Naval Oceanography Command Stennis Space Center MS 39522-5000	1
8.	Commanding Officer Fleet Numerical Oceanography Center Monterey, CA 93943-5005	1
9.	Commanding Officer Naval Ocean Research and Development Activity Stennis Space Center MS 39529-5004	1
10.	Director Naval Oceanographic and Atmospheric Research Laboratory Monterey, CA 93943-5006	1

11. Chief of Naval Research
800 North Quincy Street
Arlington, VA 22217 1

12. Office of Naval Research
Naval Ocean Research and Development Activity
800 N. Quincy Street
Arlington, VA 22217 1